mTOR controls ChREBP transcriptional activity and pancreatic β cell survival under diabetic stress

Gia Cac Chau,[1]* Dong Uk Im,[3]* Tong Mook Kang,[2] Jeong Mo Bae,[5] Won Kim,[6] Suhkneung Pyo,[4] Eun-Yi Moon,[7] and Sung Hee Um[1,3]

[1]Department of Molecular Cell Biology, Samsung Biomedical Research Institute and [2]Department of Physiology, Single Cell Network Research Center, Sungkyunkwan University School of Medicine, Suwon, Gyeonggi-do, Korea
[3]Department of Health Sciences and Technology, Samsung Advanced Institute for Health Sciences and Technology, Samsung Medical Center, Sungkyunkwan University, Seoul, Korea
[4]School of Pharmacy, Sungkyunkwan University, Suwon, Gyeonggi-do, Korea
[5]Department of Pathology, Seoul National University College of Medicine, Seoul National University Hospital and [6]Division of Gastroenterology and Hepatology, Department of Internal Medicine, Seoul National University College of Medicine, Seoul Metropolitan Government Boramae Medical Center, Seoul, Korea
[7]Department of Bioscience and Biotechnology, Sejong University, Seoul, Korea

Impaired nutrient sensing and dysregulated glucose homeostasis are common in diabetes. However, how nutrient-sensitive signaling components control glucose homeostasis and β cell survival under diabetic stress is not well understood. Here, we show that mice lacking the core nutrient-sensitive signaling component mammalian target of rapamycin (mTOR) in β cells exhibit reduced β cell mass and smaller islets. mTOR deficiency leads to a severe reduction in β cell survival and increased mitochondrial oxidative stress in chemical-induced diabetes. Mechanistically, we find that mTOR associates with the carbohydrate-response element–binding protein (ChREBP)–Max-like protein complex and inhibits its transcriptional activity, leading to decreased expression of thioredoxin-interacting protein (TXNIP), a potent inducer of β cell death and oxidative stress. Consistent with this, the levels of TXNIP and ChREBP were highly elevated in human diabetic islets and *mTOR*-deficient mouse islets. Thus, our results suggest that a nutrient-sensitive mTOR-regulated transcriptional network could be a novel target to improve β cell survival and glucose homeostasis in diabetes.

Introduction

The prevalence of diabetes, one of the most common chronic diseases worldwide, has been rising in recent decades (Kharroubi and Darwish, 2015); thus, prevention and treatment of diabetes are important issues of global healthcare. Although type 1 and type 2 diabetes are pathogenically distinct, they both exhibit chronic hyperglycemia, primarily because of impaired pancreatic β cell function and survival (Heit et al., 2006; Muoio and Newgard, 2008). Elevated blood glucose levels further induce oxidative stress and eventual β cell death (Muoio and Newgard, 2008; Shalev, 2014) and are accompanied with a progressive reduction in β cell mass (Butler et al., 2003). Thus, elucidating the molecular mechanisms responsible for maintaining β cell function and protecting against β cell death might lead to the development of novel strategies to treat diabetes.

Nutrients such as glucose and amino acids are fundamental sources for β cell growth and survival (Henquin, 2000; Xu et al., 2001; Krause et al., 2011). Under the conditions of nutrient deprivation or overload such as high-fat diet feeding, β cells maintain intracellular energy homeostasis through degradation and recycling of cellular organelles (Ebato et al., 2008; Russell et al., 2014). Indeed, markedly increased β cell apoptosis is observed in mice lacking the autophagy-related gene Atg7 (Ebato et al., 2008; Jung et al., 2008), suggesting that intracellular and extracellular nutrient status affects β cell survival and death. An important question that we have pursued is to determine how nutrient-sensitive signaling, which senses nutrient availability, is connected to β cell survival and function.

Considering that pancreatic β cells control the amounts of insulin secreted in response to nutrient levels (Muoio and Newgard, 2008; Halban et al., 2014), it is critical that they first sense extracellular glucose levels and then transduce nutrient-sensitive signals to increase insulin release and regulate their own growth. Recently, the mammalian target of rapamycin (mTOR) has emerged as a central component of nutrient sensing and cell growth (Gleason et al., 2007; Zoncu et al., 2011; Jewell and Guan, 2013; Shimobayashi and Hall, 2014). mTOR exists in two distinct complexes, mTOR complex 1 (mTORC1) and mTOR complex 2 (mTORC2; Zoncu et al., 2011). These

*G.C. Chau and D.U. Im contributed equally to this paper.

Correspondence to Sung Hee Um: shum@skku.edu; Eun-Yi Moon: eunyimoon@sejong.ac.kr

Abbreviations used: ChREBP, carbohydrate-response element–binding protein; Mlx, Max-like protein; mTOR, mammalian target of rapamycin; mTORC, mTOR complex; PARP, poly (ADP-ribose) polymerase; ROS, reactive oxygen species; STZ, streptozotocin; TXNIP, thioredoxin-interacting protein; Trx, thioredoxin.

The Rockefeller University Press
J. Cell Biol. Vol. 216 No. 7 2091–2105
https://doi.org/10.1083/jcb.201701085

two complexes share mTOR, mLST8, DEPTOR, and Tti1/Tel2 (Laplante and Sabatini, 2012). The regulatory-associated protein of mammalian target of rapamycin (raptor) and PRAS40 are known to be components of mTORC1, whereas rapamycin-insensitive companion of mTOR (rictor), mSin1, and protor1/2 are components of mTORC2 (Laplante and Sabatini, 2012).

Details of the molecular mechanisms of by which nutrients are sensed inside cells through mTOR signaling pathway are beginning to emerge (Shimobayashi and Hall, 2014; Chantranupong et al., 2016; Wolfson et al., 2016). When amino acids such as glutamine and arginine are abundant, vacuolar H^+-ATPase stimulates guanine exchange factor activity of Ragulator, a complex encoded by the *MAPKSP1*, *ROBLD3*, and *c11orf59* genes (Sancak et al., 2010), and inhibits the GTPase activating protein activity of GTPase activating protein activity toward Rags 1 (Bar-Peled et al., 2013), leading to the formation of heterodimeric complex RagA.B-GTP/RagC.D-GDP (Rag GTPase; Sancak et al., 2008). Activated Rag GTPase binds to and recruits mTORC1 to the lysosome surface, where its kinase activator, Rheb, a small GTPase, resides (Bar-Peled et al., 2012; Chantranupong et al., 2016). In leucine-induced mTOR activation, leucyl-tRNA synthetase directly binds to Rag GTPase to induce the binding of Rag GTPase to mTOR, leading to the recruitment of mTOR to the lysosome surface (Han et al., 2012), suggesting that multiple signaling components signal to mTORC1 complex for amino acid sensing.

Consistent with the roles of mTORC1 in nutrient-sensitive responses, mice injected with rapamycin, which inhibits mTORC1 activity, display reduced β cell mass and glucose intolerance (Houde et al., 2010). In addition, mice lacking S6K1, a downstream effector of mTORC1, display hypoinsulinemia, decreased β cell size, and enhanced insulin sensitivity (Pende et al., 2000; Um et al., 2004). We further demonstrated that nutrient-sensitive S6K1 in β cells is critical to β cell growth during the development and adult period in a cell-autonomous manner (Um et al., 2015). Moreover, offspring of dams exposed throughout pregnancy to a low-protein diet, which also reduces mTORC1 activity, exhibit impaired glucose tolerance (Alejandro et al., 2014). As adults, the normal phenotype can be rescued by activation of mTORC1 signaling, indicating that mTORC1 signaling actively controls β cell growth and programming during fetal development and adult life (Alejandro et al., 2014). In addition to mTORC1, mice expressing kinase-dead Akt, a downstream target of mTORC2 in β cells, exhibit glucose intolerance and decreased insulin secretion (Bernal-Mizrachi et al., 2004). Similarly, the loss of rictor, a crucial component of mTORC2, leads to a reduction in Akt activity in β cells and results in mild hyperglycemia, reduced β cell mass, and defective insulin secretion (Gu et al., 2011). Thus, these studies suggest that downstream effectors or components of mTOR complexes such as S6K1, Akt, and rictor are critical to β cell growth, proliferation, and function.

The individual roles of downstream effectors and components of mTORC1 and mTORC2 in β cells have been determined through analysis of mice lacking S6K1, Akt, rictor, and TSC1/2 or through analysis of mice treated with rapamycin (Pende et al., 2000; Bernal-Mizrachi et al., 2004; Mori et al., 2009; Houde et al., 2010; Gu et al., 2011; Koyanagi et al., 2011; Um et al., 2015). However, the physiological function of mTOR, a central component of mTORC1 and mTORC2 in β cells, has not been elucidated, primarily because knockout of the mouse mTOR gene results in embryonic lethality (Gangloff et al., 2004; Murakami et al., 2004). Here, we analyzed pancreatic β cell–specific mTOR deficiency and determined how mTOR regulates nutrient and stress-sensitive β cell survival and function physiologically. Moreover, we have evaluated the clinical relevance of our findings in human diabetic islets. Considering the implication of thioredoxin-interacting protein (TXNIP) on pancreatic β cell death under oxidative stress and diabetic conditions (Chen et al., 2008; Lerner et al., 2012; Oslowski et al., 2012) and the impact of mTORC1 signaling on TXNIP expression in response to glucose and glutamine stimulation (Kaadige et al., 2015), we further examined whether mTOR regulates TXNIP expression in pancreatic β cells under the condition of diabetes.

Results

β Cell–specific deficiency of mTOR leads to a reduction in islet size and β cell mass

β Cell–specific *mTOR* deficient mice (*βmTORKO*) were generated by crossing $mTOR^{flox/flox}$ mice (*WT*; Gangloff et al., 2004; Murakami et al., 2004) with transgenic mice expressing Cre recombinase under the control of the rat insulin II promoter (*RIP-Cre* mice; Fig. S1 A). The deficiency of mTOR was confirmed in primary mouse islets (Fig. 1 A). However, we did not detect significant differences in mRNA and protein levels of mTOR in the hypothalamus between *βmTORKO* and *WT* mice (Figs. 1 A and S1 B), indicating β cell–specific mTOR deletion. *βmTORKO* mice displayed no difference in body weight and blood glucose compared with *WT* mice (Figs. 1 B and S1 C). To examine the role of mTOR in systemic glucose homeostasis, we performed glucose tolerance test and insulin tolerance test. *βmTORKO* mice displayed mild glucose intolerance and insulin resistance compared with *WT* mice (Fig. 1, C and D). Although the levels of serum insulin were similar between *βmTORKO* and *WT* mice that were fed standard chow ad libitum (Fig. 1 E), the levels of insulin secretion during glucose tolerance tests were markedly reduced in *mTOR*-deficient mice (Fig. 1 F). These results suggest that mTOR plays a role in maintaining glucose homeostasis. To understand how *βmTORKO* mice exhibit glucose intolerance and insulin resistance, we examined the islet morphology and β cell mass by hematoxylin and eosin staining and immunohistochemistry. Hematoxylin and eosin staining analysis indicated that the mean islet volume in *βmTORKO* mice was significantly reduced compared with those in *WT* mice (299 ± 55 in *βmTORKO* vs. $670 \pm 63 \times 10^3$ μm^3 in *WT*, $P < 0.05$; Fig. 1 G). Consistent with this, the relative β cell mass was significantly decreased in *βmTORKO* mice (1.66 ± 0.3 in *βmTORKO* vs. 3.2 ± 0.4 mg in *WT*, $P < 0.05$; Fig. 1 H). We next examined how mTOR deficiency affects β cell mass, we assessed β cell replication by performing immunohistochemistry for Ki67, a nuclear protein marker of proliferating cells, and β cell apoptosis using TUNEL assay. There was no difference in β cell replication between *WT* and *βmTOR KO* mice (1.5 ± 0.3 in *βmTORKO* vs. $1.1 \pm 0.3\%$ in *WT*, $P < 0.1$; Fig. 1 I). However, TUNEL staining demonstrated an increase of β cell death in *βmTORKO* mice (2.3 ± 0.3 in *βmTOR KO* vs. $1.1 \pm 0.2\%$ in *WT*, $P < 0.05$; Fig. 1 J), suggesting a protective role of mTOR in maintaining β cell mass. Together, these results suggest that mTOR plays a critical role in the regulation of islet growth and β cell mass.

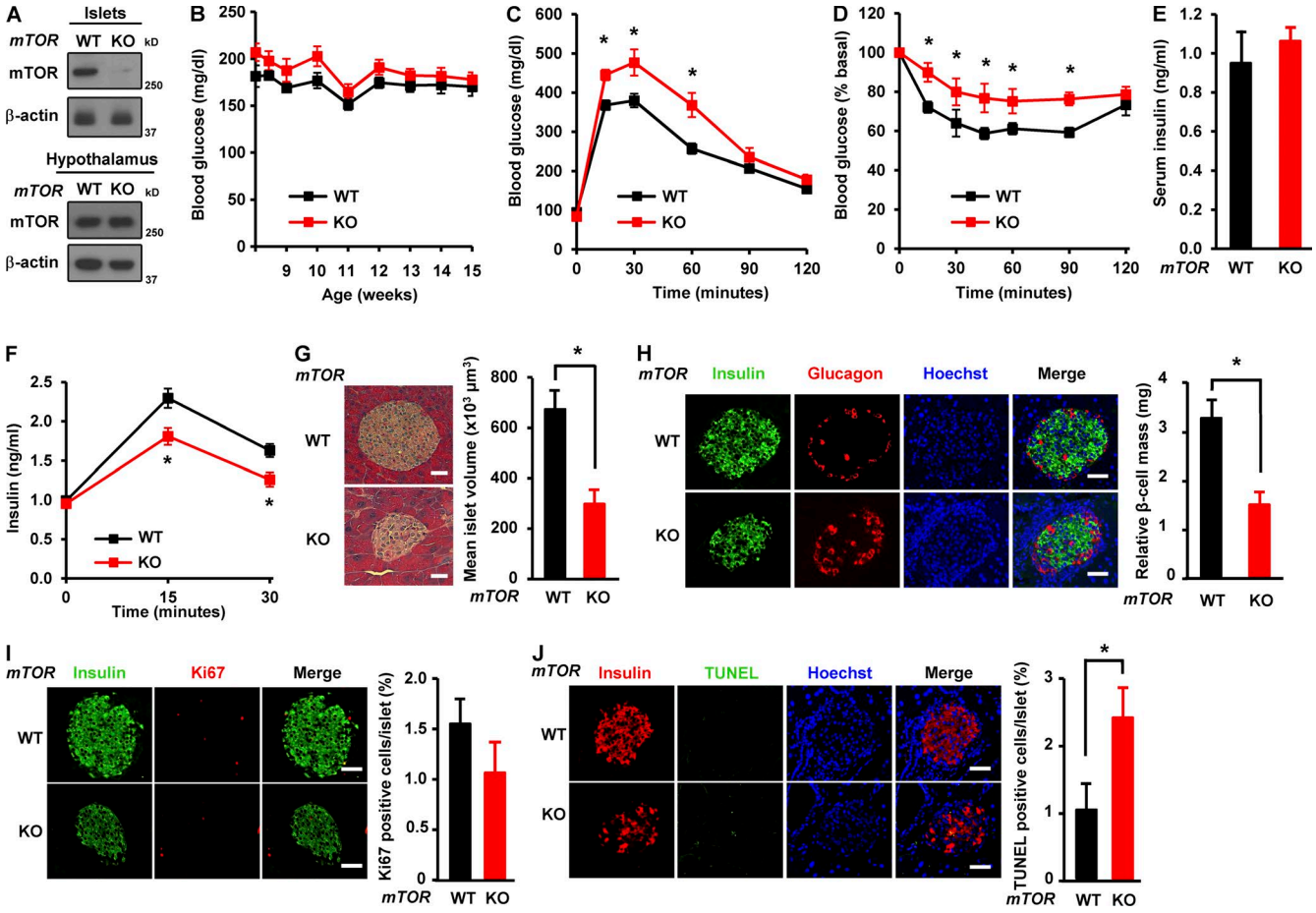

Figure 1. **β Cell–specific deficiency of mTOR leads to reduction in islet size and β cell mass.** (A) Immunoblots showing mTOR expression in isolated islets and hypothalamus from *WT* (*mTOR*$^{flox/flox}$) or *βmTOR knockout* (*KO*) mice (*mTOR*$^{flox/flox}$*RIP Cre*). (B) Blood glucose levels were monitored weekly for 8 wk. (C) Glucose tolerance tests were performed in 12-wk-old mice (2 g glucose per kilogram body weight). (D) Insulin tolerance tests were performed in 12-wk-old mice (0.75 U insulin per kilogram body weight). (E) Serum insulin levels in 12 wk-old *WT* and *mTOR*-deficient mice fed standard chow. In B–E, *WT*, *n* = 8; *knockout*, *n* = 6. (F) Serum insulin levels were measured during glucose tolerance testing (*WT*, *n* = 7; *knockout*, *n* = 6). (G, left) Representative hematoxylin and eosin staining of pancreatic sections from *WT* and *βmTORKO* mice. Bars, 75 µm. (right) Mean islet volume was calculated in hematoxylin and eosin–stained pancreatic sections. (H, left) Immunofluorescence staining for insulin (green) or glucagon (red) in *WT* and *βmTORKO* mice; Nuclei are shown with Hoechst (blue) staining. Bars, 50 µm. (right) Relative β cell mass. (I) β Cell proliferation in *WT* and *βmTORKO* mice. (left) Representative immunofluorescence images of pancreatic sections from *WT* and *βmTORKO* mice using antibodies against insulin (green) or Ki67 (red). Bars, 50 µm. (right) β Cell proliferation was quantified by percentage of Ki67-positive cells. (J, left) Representative immunofluorescence images of mouse islets stained for TUNEL (green), or insulin (red). Nuclei are stained blue with Hoechst. Bars, 50 µm. (right) Quantification of TUNEL-positive islets in pancreatic sections. In G–J, 18 sections from six *WT* mice and 15 sections from five *knockout* mice were stained. In B–J, values are given as mean ± SEM. *, P < 0.05 versus *WT* (ANOVA).

mTOR deficiency leads to impaired nutrient dependent insulin secretion in β cells

In view of the defect in glucose-induced insulin secretion in *βmTORKO* mice in vivo (Fig. 1 F), we next determined whether mTOR deficiency or depletion affected glucose-stimulated insulin secretion ex vivo and in vitro, and we determined whether such effects were developmentally related. mTOR deficiency was achieved in isolated *mTOR*$^{flox/flox}$ islets by infection with adenovirus expressing Cre (Ad-Cre; Fig. 2 A). *mTOR*-deficient islets exhibited 31.2% less insulin secretion compared with *WT* islets (Fig. 2 B). Given that glucose triggers insulin secretion in pancreatic β cells by increasing ATP content and enhancing Ca^{2+} influx, eventually leads to exocytosis of insulin granules, we measured the ADP/ATP ratio in islets. mTOR deficiency in islets led to increased ADP/ATP ratio after either low- or high-glucose treatment, compared with *mTOR*$^{flox/flox}$ islets infected with adenovirus expressing GFP (Ad-GFP; Fig. 2 B). Consistent with this, reducing mTOR levels resulted in decreased insulin secretion and elevated ADP/ATP ratios in INS-1 cells upon either low- or high-glucose stimulation (Fig. 2 C). Similarly, the inhibition of mTORC1 activity by rapamycin or the inhibition of both mTORC1 and mTORC2 activities by PP242 led to decreased insulin secretion (Fig. 2 D) and increased ADP/ATP ratios upon low- or high-glucose treatment (Fig. 2 E). Considering that the rise of intracellular free Ca^{2+} is critical for inducing exocytosis of insulin granules (Henquin, 2000; Muoio and Newgard, 2008), we measured intracellular free Ca^{2+} concentration in islets. *mTOR*-deficient islets exhibited lower increase of intracellular Ca^{2+} levels than *mTOR*$^{flox/flox}$ islets in response to glucose stimulation (Fig. 2 F). We further determined whether mTOR deficiency was associated with defects in mitochondrial membrane potential, which are connected to ATP generation and eventual insulin secretion (Maechler, 2013). The mitochondrial membrane potential was significantly reduced in *mTOR*-deficient islets (Fig. 2 G) and mTOR-depleted cells (Fig. 2 H). Consistent with this, analysis of oxygen consumption rate

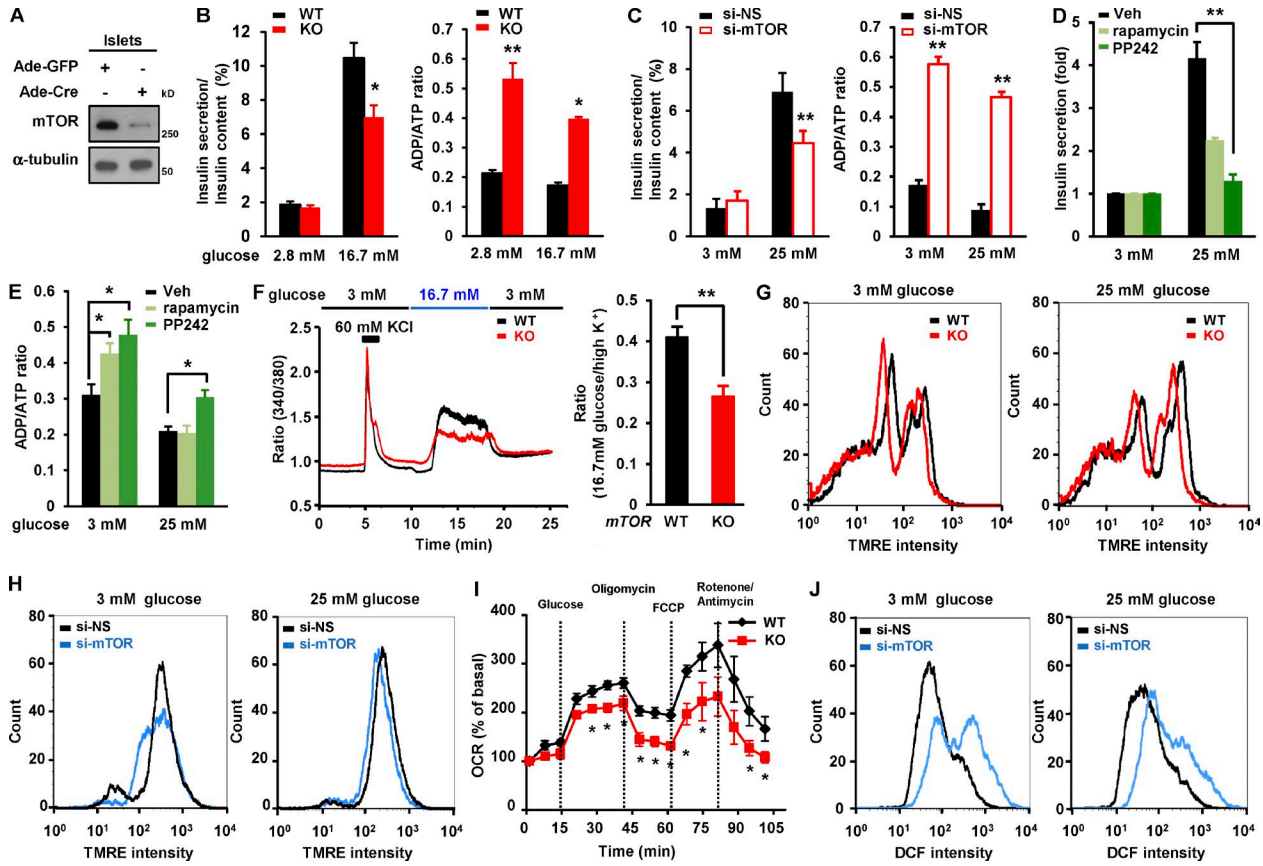

Figure 2. **mTOR deficiency in β cells leads to impaired nutrient dependent insulin secretion in β cells.** (A) Immunoblots showing deletion of mTOR in primary islets. Isolated islets were infected with either Ad-GFP or Ad-Cre at an MOI of 25 for 48 h. (B) Glucose-stimulated insulin secretion and ADP/ATP ratio in *WT* and *mTOR*-deficient islets ($n = 4$ per group). (C) Insulin secretion and ADP/ATP ratio after mTOR depletion. INS-1 cells transfected with 10 nM si-NS or si-mTOR were incubated with 3 mM glucose or 25 mM glucose in KRBH buffer for 1 h. (D) Insulin secretion in rapamycin- or PP242-treated cells. INS-1 cells were treated with either 20 nM rapamycin or 1 µM PP242 for 24 h. (E) ADP/ATP ratio in rapamycin- or PP242-treated cells. (F) Glucose-induced Ca^{2+} influx in *WT* and *mTOR*-deficient islets. Representative trace (left) and quantification of $[Ca^{2+}]_i$ with Fura-2 (right) in isolated islets stimulated with the indicated amounts of glucose ($n = 5$ per group). (G) Mitochondrial membrane potential in *WT* and *mTOR*-deficient islets (*WT*, $n = 5$; knockout [*KO*], $n = 4$). (H) Mitochondrial membrane potential in INS-1 cells after mTOR depletion. (I) Oxygen consumption rate (OCR) was measured in *mTOR*-deficient islets ($n = 5$ per group). (J) Histogram showing ROS levels in INS-1 cells after mTOR knockdown. In C, D, E, H, and J, $n = 3$ independent experiments; values are given as mean ± SEM. In C, D, and E, *, $P < 0.05$; **, $P < 0.01$ versus control (si-NS or vehicle; ANOVA). In B, F, and I, *, $P < 0.05$; **, $P < 0.01$ versus *WT* (ANOVA). DCF, Dicholorofluorescein; TMRE, tetramethylrhodamine ethyl ester; Veh, vehicle.

indicated that mitochondrial respiration in *mTOR*-deficient islets was reduced in response to high-glucose challenge (Fig. 2 I). Given that the levels of reactive oxygen species (ROS) affect mitochondrial ATP production and insulin release in β cells upon glucose treatment (Sakai et al., 2003), we further examined the levels of ROS after mTOR knockdown. The generation of ROS induced by glucose stimulation in mTOR depleted cells was increased by 62% compared with control cells upon glucose stimulation (Fig. 2 J), suggesting that mTOR deficiency–mediated decreases in mitochondrial membrane potential and increases in ROS production are associated with a reduction in mitochondrial activity. Thus, these results suggest that mTOR plays a positive role in insulin secretion: regulating ADP/ATP ratios, maintaining mitochondrial membrane potential, enhancing Ca^{2+} influx, and suppressing ROS generation in β cells.

Deletion of mTOR in pancreatic β cells exacerbates the development of chemically induced diabetes

The impaired β cell function and survival are commonly characterized in diabetes (Muoio and Newgard, 2008). Streptozotocin (STZ) has been extensively used to induce diabetic mimetic condition and β cell death (Chen et al., 2008; Lee et al., 2016). To determine the consequence of mTOR deficiency on β cell survival in chemically induced diabetes, we injected STZ (100 mg/kg body weight; i.p.) or vehicle into *WT* and *βmTORKO* mice twice a week for 2 wk. Mice were fed normal chow ad libitum throughout. Body weight and blood glucose were monitored for 8 wk after STZ injection. Under these conditions, *βmTORKO* mice exhibited a 17.8% reduction in body weight compared with *WT* mice (Fig. S1 D). In addition, the levels of blood glucose in *βmTORKO* mice were markedly increased compared with those in *WT* mice (Fig. 3 A). We next examined how mTOR regulates systemic glucose homeostasis in chemically induced diabetes. *βmTORKO* mice displayed very severe glucose intolerance compared with *WT* mice (Fig. 3 B). High blood glucose levels in these *βmTORKO* mice were accompanied by insulin resistance (Fig. 3 C) and significantly reduced insulin levels compared with *WT* mice (Fig. 3 D) and were also accompanied by decreased glucose-induced insulin secretion in vivo (Fig. 3 E). These results suggest that mTOR plays a critical role in maintaining glucose homeostasis in diabetes. Consistent with this, mean islet volume was strikingly decreased in *βmTOR KO* mice after STZ injection (166 ± 14 in *βmTORKO* vs. 337

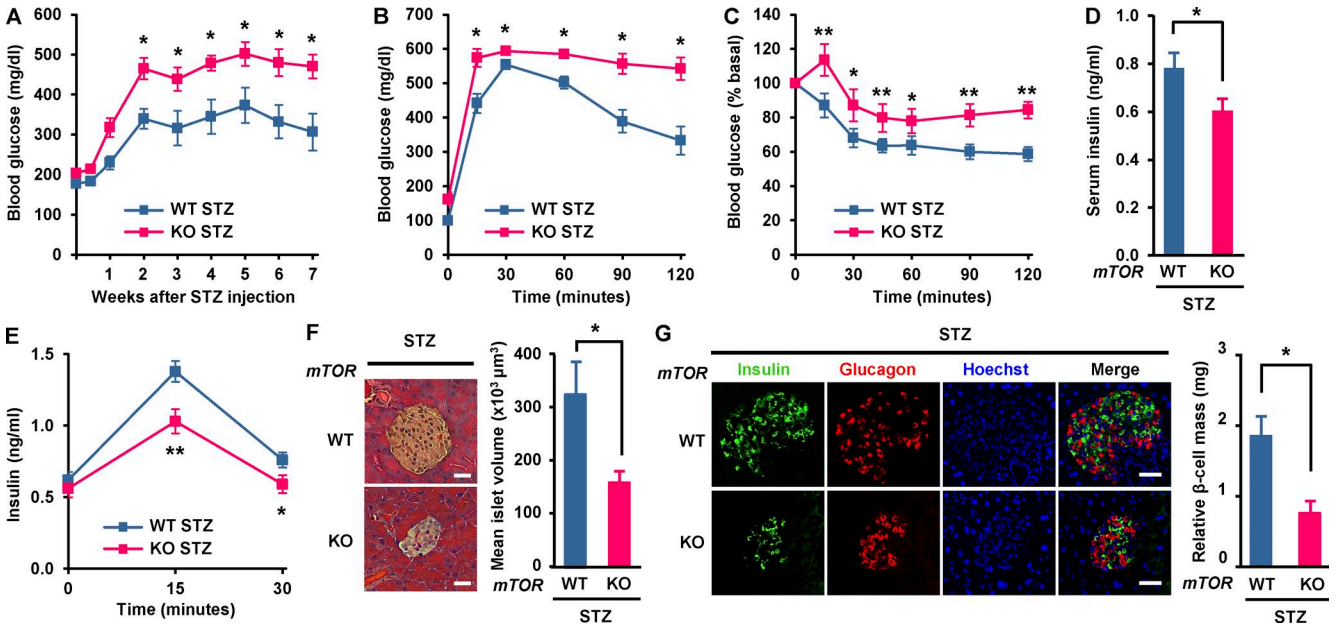

Figure 3. **Deletion of mTOR in pancreatic β cells exacerbates the development of chemically induced diabetes.** Vehicle (Veh) or STZ (100 mg/kg body weight) were administered twice a week for 2 wk. (A) Blood glucose levels were monitored weekly for 8 wk after STZ administration. (B) Glucose tolerance tests were performed 21 d after STZ injection. (C) Insulin tolerance tests were performed 21 d after STZ injection. (D) Serum insulin levels were measured in random fed *WT* and *mTOR*-deficient mice 21 d after STZ injection. In A–D, *WT, n* = 8; knockout [*KO*], *n* = 6. (E) Insulin secretion measured during glucose tolerance testing (*WT, n = 7; knockout, n* = 6). (F, left) Representative hematoxylin and eosin staining of pancreatic sections from *WT* and *βmTORKO* mice 8 wk after STZ injection. Bars, 75 µm. (right) Mean islet volume was calculated in hematoxylin and eosin–stained pancreatic sections. (G) β Cell number in *WT* and *βmTORKO* mice upon STZ exposure. (left) Immunofluorescence staining for insulin (green), or glucagon (red). Nuclei are shown with Hoechst (blue) staining. Bars, 50 µm. (right) Relative β cell mass. In F and G, 18 sections from six *WT* mice and 15 sections from five knockout mice were stained. In A–G, values are given as mean ± SEM. *, P < 0.05; **, P< 0.01 versus *WT* (ANOVA).

± 45 × 10^3 µm^3 in *WT*, P < 0.05; Fig. 3 F). Moreover, the relative β cell mass was significantly decreased in *βmTORKO* mice compared with *WT* mice (0.7 ± 0.2 in *βmTORKO* vs. 1.83 ± 0.33 mg in *WT*, P < 0.05; Fig. 3 G), suggesting that mTOR provides some level of protection against loss of β cells in diabetic animals. Significant reduction of β cell mass and islet size in *βmTORKO* mice under diabetic conditions might be connected with severe glucose intolerance and reduced insulin secretion.

mTOR protects β cell survival in STZ-induced diabetes

We next examined how mTOR regulates replication and β cell survival upon STZ-induced diabetes. The density of Ki67-positive β cells islets was dramatically lower in *βmTORKO* islets (0.8 ± 0.2 in *βmTORKO* vs. 2.9 ± 0.6% in *WT*, P < 0.05; Fig. 4 A). The increase in Ki67-positive cells in *WT* mice under STZ treatment suggests that β cells in these mice tend to proliferate more than normal to overcome cell loss under diabetic conditions. In addition, TUNEL assay revealed that the rate of β cell apoptosis was significantly greater in *βmTORKO* mice than in *WT* mice (6.3 ± 0.7 in *βmTORKO* vs. 3.4 ± 0.5% in *WT*, P < 0.01; Fig. 4 B). This suggests that β cell survival in diabetes is dependent on mTOR. Moreover, the decrease in mean islet volume (Fig. 3 F) and relative β cell mass (Fig. 3 G) and the increase in the rate of β cell apoptosis (Fig. 4 B) in *βmTOR KO* mice were much more severe in the diabetic condition than in the normal condition (Fig. 1, G, H, and J), suggesting that mTOR is more critical for protecting β cells under diabetic conditions. To determine whether β cells require mTOR for their survival independently of the humoral environment, we assessed the effect of in vitro STZ treatment on *βmTORKO* islets (Fig. 4 C) and on mTOR knockdown INS-1 cells (Fig. 4 D). In both *βmTORKO* islets and mTOR knockdown INS-1 cells, such treatment resulted in a dramatic increase in the expression of apoptosis-related proteins such as cleavage of poly (ADP-ribose) polymerase (PARP) and Bcl-2–associated X protein (Bax; Fig. 4, C and D). Consistent with this, the percentage of cells in sub-G1 phase was increased in STZ-treated mTOR knockdown cells (Fig. 4 E). Given that mitochondria appear to be highly sensitive to oxidative and apoptotic stress (Yano et al., 2011; Maechler, 2013), we analyzed mitochondrial membrane potential and generation of ROS. Mitochondrial membrane potential was dramatically decreased in *mTOR*-deficient islets in diabetes (Fig. 4 F). Consistently, generation of ROS was markedly increased in mTOR-depleted INS-1 cells after STZ treatment (Fig. 4 G), suggesting that mTOR plays a protective role against oxidative stress-induced mitochondrial toxicity in β cells.

mTOR deficiency induces expression of TXNIP and ChREBP in β cells upon metabolic stress

We next addressed the molecular mechanism by which mTOR regulates β cell survival. In diabetes mellitus, glucotoxicity is one of the critical factors involved in β cell death (Muoio and Newgard, 2008). Given that TXNIP, a key modulator of the redox system (Shalev, 2014), induces ROS generation and cell death in β cells (Oslowski et al., 2012), we assessed mRNA expression levels of TXNIP in *mTOR*-deficient β cells and INS-1 cells upon high-glucose treatment. Levels of TXNIP mRNA were increased in *mTOR*-deficient islets and mTOR knockdown INS-1 cells (Figs. 5 A and S2 A). Considering that the expression of

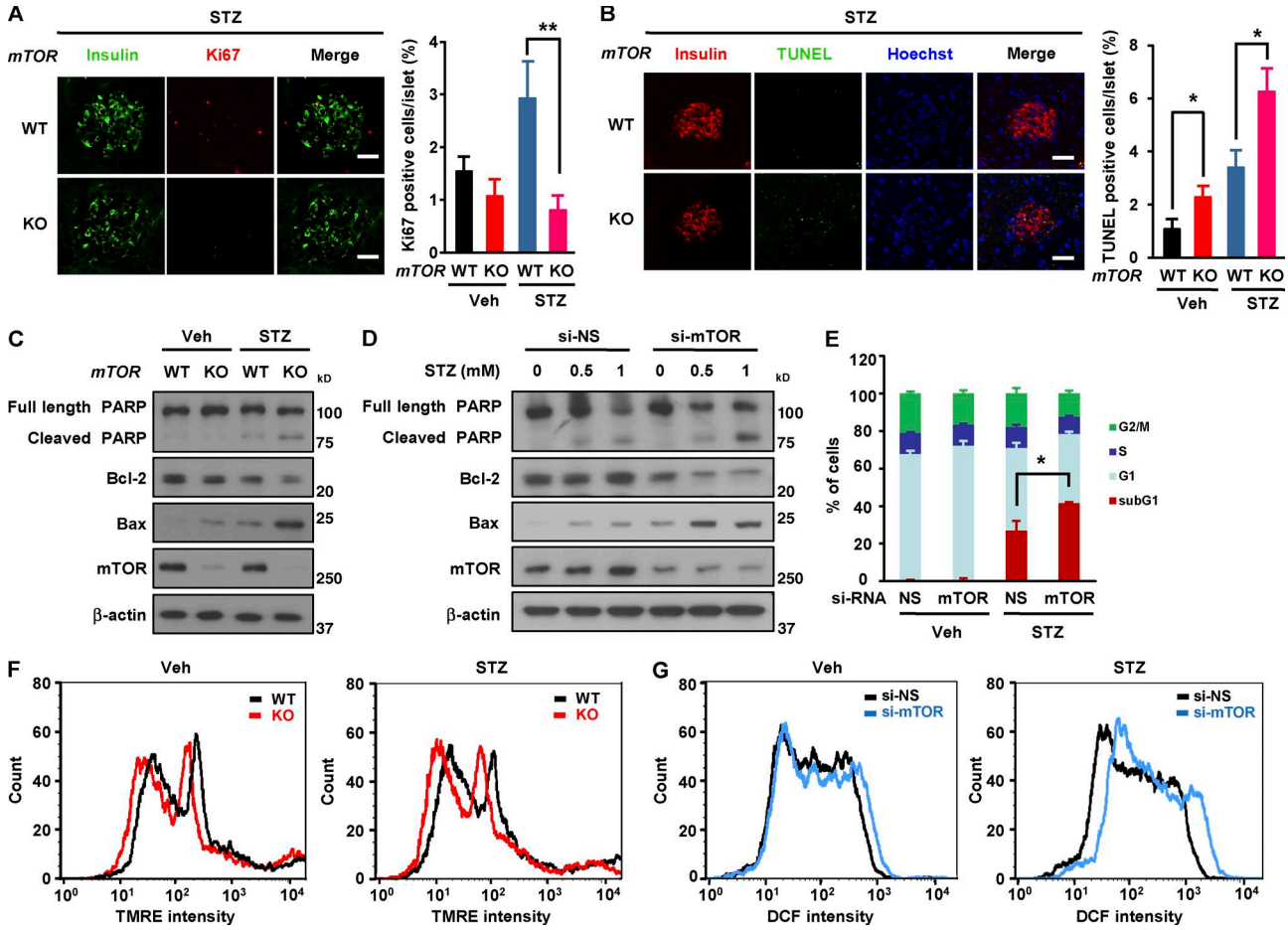

Figure 4. **mTOR protects β cell survival in STZ-induced diabetes.** (A, left) β Cell proliferation in *WT* and *βmTORKO* mice after 8 wk of STZ injection. Representative immunofluorescence images of pancreatic sections from *WT* and *βmTORKO* mice using antibodies against insulin (green) or Ki67 (red). (right) β Cell proliferation was quantified by percentage of Ki67-positive cells. Data for Veh group is from Fig. 1 I. (B, left) Representative immunofluorescence images of mouse islets stained for TUNEL (green), or insulin (red) 8 wk after STZ injection. Nuclei are stained blue with Hoechst. (right) Quantification of TUNEL positive islets in pancreatic sections. Data for Veh group is from Fig. 1 J. Bars, 50 µm. 18 sections from six *WT* mice and 15 sections from five *knockout* mice were stained. (C) Expression of apoptosis-related proteins in mouse islets after 1 mM STZ treatment for 6 h (n = 4 per group). (D) Expression of apoptosis-related proteins in INS-1 cells after treatment with 1 mM STZ. (E) Percentage of sub-G1 phase cells after mTOR depletion under STZ exposure (n = 5 per group). (F) Mitochondrial membrane potential in *WT* and *mTOR*-deficient islets after STZ treatment (n = 5 per group). (G) ROS levels after mTOR knockdown after STZ treatment (n = 3). In A, B, and E, values are given as mean ± SEM. *, $P < 0.05$ versus control (*WT* or si-NS); **, $P < 0.01$ versus *WT* (ANOVA).

TXNIP is transcriptionally regulated by carbohydrate-responsive element–binding protein (ChREBP) in β cells (Cha-Molstad et al., 2009; Kibbe et al., 2013), we next examined mRNA expression levels of ChREBP upon high-glucose treatment. The levels of ChREBP mRNA were increased in *mTOR*-deficient islets and mTOR knockdown INS-1 cells (Figs. 5 A and S2 A). Consistent with this, TXNIP and ChREBP protein levels were increased by deficiency of mTOR or inhibition of its activity using rapamycin or PP242 in response to high glucose (Fig. 5 B and Fig. S2, B and C), suggesting that lack of mTOR or inhibition of its activity up-regulates the expression of TXNIP and ChREBP. However, the expression levels of TXNIP and ChREBP in the hypothalamus were similar between *βmTORKO* and *WT* mice (Fig. S2 D). We further assessed whether deficiency or depletion of mTOR affects TXNIP and ChREBP expression in mouse islets or INS-1 cells upon STZ treatment. The levels of TXNIP and ChREBP mRNA in *mTOR*-deficient islets and mTOR-depleted cells were markedly increased compared with *WT* islets and nonsilencing siRNA transfected cells, respectively (Fig. 5 C and S2 E). Similarly, TXNIP and ChREBP protein levels were increased in *mTOR* deficient islets (Fig. 5 D), mTOR knockdown cells (Fig. S2 F), and rapamycin or PP242 treated cells (Fig. S2 G) under STZ exposure. To further determine β cell specific up-regulation of TXNIP and ChREBP under the diabetic condition, we performed double immunostaining of TXNIP and insulin or ChREBP and insulin in pancreatic sections from *WT* and *βmTORKO* mice injected with either vehicle or STZ. This analysis showed that TXNIP was stained strongly in β cells of *βmTORKO* mice and was increased further upon STZ treatment (Fig. 5 E). Similar to TXNIP, ChREBP signals were also higher in islets of *βmTORKO* mice and diabetic mice (Fig. 5 F). Conversely, the overexpression of wild-type mTOR, but not kinase-dead mTOR, attenuated the expression of TXNIP and ChREBP after STZ treatment, indicating that the activity of mTOR regulates TXNIP and ChREBP expression (Fig. 5 G). Moreover, overexpression of mTOR restored Bcl-2 expression levels, prevented an increase in Bax expression (Fig. 5 H), and abolished the STZ-induced increase in the percentage of cells in sub-G1 phase (Fig. S2 H).

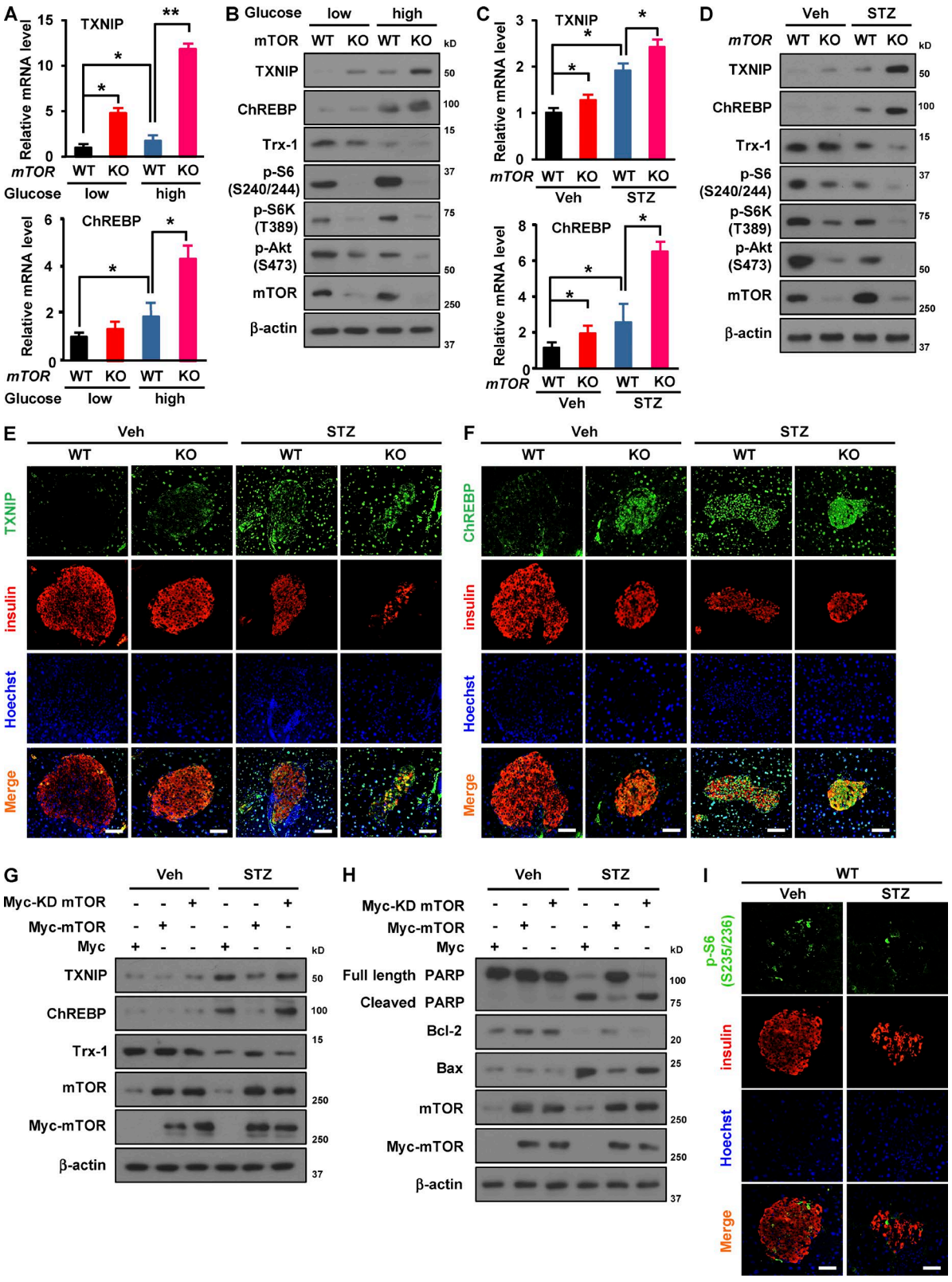

Figure 5. **Deficiency of mTOR induces expression of TXNIP and ChREBP in β cells upon metabolic stress.** (A) TXNIP and ChREBP mRNA levels in *WT* and *mTOR*-deficient islets after low- (5 mM) or high-glucose (25 mM) treatment. (B) Immunoblots showing TXNIP and ChREBP expression in mouse islets under high-glucose treatment. (C) mRNA levels of TXNIP and ChREBP in *WT* and *mTOR*-deficient islets after STZ treatment. (D) Immunoblots showing TXNIP and ChREBP expression in mouse islets upon STZ treatment. In A–D, *WT*, $n = 6$; knockout (*KO*), $n = 5$. (E and F) Expression levels of TXNIP and ChREBP in *WT* and *βmTORKO* islets upon STZ exposure. Representative immunofluorescence images of pancreatic sections from *WT* mice after 8 wk of STZ injection using antibodies against TXNIP (green; E) or ChREBP (green; F) and insulin (red). Nuclei are shown with Hoechst (blue) staining. (G) Immunoblots showing expression of TXNIP and ChREBP in mTOR-overexpressing cells after STZ treatment. (H) Immunoblots showing levels of apoptosis-related proteins in mTOR-overexpressing cells. Myc-KD mTOR, Myc-kinase dead mTOR. (I) Phosphorylation of S6 protein (p-S6 Ser 235/236) upon STZ treatment. Representative

TXNIP interacts with and inhibits the activity of thioredoxin-1 (Trx-1), an antioxidant molecule, which has a critical role in protecting β cells from oxidative stress (Huh et al., 2013). We next examined levels of Trx-1 in *mTOR*-deficient islets or mTOR knockdown INS-1 cells. Deletion or depletion of mTOR resulted in decreased Trx-1 expression after high-glucose treatment (Figs. 5 B and S2 B) or STZ treatment (Figs. 5 D and S2 F). In contrast, overexpression of mTOR abolished the oxidative stress–induced decrease in Trx-1 expression (Fig. 5 G), suggesting that mTOR protects against β cell death via the Trx-1–TXNIP axis. We further determined whether mTORC1 or mTORC2 regulates TXNIP transcription upon high-glucose or STZ treatment. Under these conditions, expression of TXNIP in INS-1 cells was increased by depletion of raptor, but not rictor (Fig. S2, I and J), indicating a role of mTORC1 in regulating TXNIP expression. Consistent with this, immunostaining analysis indicated that levels of S6 phosphorylation (Ser 235/236) were markedly decreased in response to STZ exposure (Fig. 5 I), along with a decrease in mTOR phosphorylation (Ser 2448; Fig. S2 K), suggesting that mTORC1 activity was reduced by STZ treatment.

mTOR is associated with glucose-responsive ChREBP, leading to suppression of TXNIP expression

We have shown that deficiency or depletion of mTOR induced the expression of TXNIP and ChREBP upon high-glucose treatment or STZ exposure (Figs. 5 and S2), suggesting that mTOR suppresses ChREBP-mediated transcription of TXNIP upon nutritional or apoptotic stress. To confirm whether mTOR regulates TXNIP transcription through ChREBP in β cells, we depleted ChREBP in INS-1 cells. Reducing ChREBP levels abolished mTOR deficiency–induced up-regulation of TXNIP expression upon high-glucose treatment (Fig. 6 A), suggesting that mTOR suppresses TXNIP expression through ChREBP. To determine whether mTOR inhibits binding of ChREBP to the TXNIP promoter, we performed a chromatin immunoprecipitation assay. The binding of ChREBP to the ChoRE region of the TXNIP promoter was enhanced by mTOR depletion under the low-glucose condition, and such binding was further increased by high-glucose treatment (Fig. 6 B). Similarly, reducing ChREBP levels abolished mTOR deficiency–induced up-regulation of TXNIP expression upon STZ treatment (Fig. 6 C). A chromatin immunoprecipitation assay demonstrated that the binding of ChREBP to the ChoRE region of the TXNIP promoter was enhanced by mTOR depletion, and the enhanced binding was further increased by STZ treatment (Fig. 6 D). These results indicate that mTOR inhibits the binding of ChREBP to the TXNIP promoter, eventually leading to the suppression of TXNIP expression.

ChREBP associates with Max-like protein (Mlx), and the complex is known to act as a transcriptional regulator of TXNIP in INS-1 cells upon high-glucose stimulation (Cha-Molstad et al., 2009). Considering that expression levels of TXNIP and ChREBP were increased after treatment with high glucose or STZ (Fig. 5), we assessed binding of ChREBP to Mlx. Immunoprecipitation analysis revealed that the association of ChREBP with Mlx was enhanced by STZ treatment (Fig. 6 E), suggesting that formation of the ChREBP–Mlx complex was increased in response to STZ. Given that ChREBP is required for TXNIP transcription (Cha-Molstad et al., 2009; Fig. 6, B and D) and mTOR suppresses TXNIP expression (Fig. 5), we examined whether mTOR directly binds to ChREBP. Notably, we found that ChREBP was coimmunoprecipitated with mTOR and that STZ treatment increased the relative amount of ChREBP in the precipitate (Fig. 6 F). Based on our results showing that ChREBP and Mlx form a complex (Fig. 6 E) and mTOR binds to ChREBP (Fig. 6 F), we next investigated whether mTOR also interacted with Mlx. We found that mTOR was associated with Mlx, and the association was increased by STZ treatment (Fig. 6 F), suggesting that mTOR interacts with the ChREBP–Mlx complex under apoptotic stress conditions. Given that two ChREBP–Mlx complexes bind to the two E boxes of the ChoRE motif to provide a positive transcriptional input to TXNIP expression (Cha-Molstad et al., 2009), our results suggest that mTOR regulates the formation of the ChREBP–Mlx complex for the transcription of TXNIP (Fig. 6, B and D). We further examined whether mTOR affects the association between ChREBP and Mlx. Binding between ChREBP and Mlx was increased by mTOR depletion (Fig. 6 G), suggesting that mTOR negatively regulates the association of ChREBP and Mlx. Together, these results suggest that mTOR suppresses TXNIP expression via inhibiting the transcriptional activity of ChREBP.

The expression levels of TXNIP and ChREBP are elevated in human diabetic islets

Based on the fact that the ChREBP–Mlx complex translocates from the cytoplasm into the nucleus, where it binds to the ChoRE region of the TXNIP promoter to induce TXNIP transcription (Cha-Molstad et al., 2009), we next determined whether mTOR is involved in nuclear translocation of the ChREBP–Mlx complex to induce TXNIP transcription with STZ treatment. In vehicle-treated cells, mTOR, ChREBP, and Mlx were separated in the cytoplasm (Fig. 7, A–C). In contrast, in the chemically induced diabetic condition, mTOR was associated with ChREBP and Mlx in the cytoplasm, but not in the nucleus (Fig. 7, A and B). This tells us that mTOR does not translocate together with the ChREBP–Mlx complex from the cytoplasm into the nucleus but rather regulates the binding of ChREBP–Mlx to the TXNIP promoter under STZ treatment. We further examined whether depletion of mTOR affects the translocation of ChREBP–Mlx complex into the nucleus under such conditions. The depletion of mTOR induced the translocation of the ChREBP–Mlx complex into the nucleus after STZ exposure, suggesting that mTOR inhibits the translocation of the ChREBP–Mlx complex under apoptotic stress conditions (Fig. 7 C). The levels of ChREBP were elevated in the nucleus of mTOR-depleted cells upon STZ treatment (Figs. 7 C and S2 L). To evaluate the clinical relevance of TXNIP and ChREBP in diabetes, we assessed the expression levels of these proteins in human diabetic islets by immunostaining. The levels of TXNIP and ChREBP expression were significantly elevated in islets from subjects with diabetes compared with nondiabetic subjects

immunofluorescence images of pancreatic sections from *WT* mice after 8 wk of STZ injection using antibodies against p-S6 (Ser 235/236) (green) and insulin (red). Nuclei are shown with Hoechst (blue) staining. In E, F, and I, bars, 50 µm; *WT*, $n = 6$; *knockout*, $n = 5$. In A and C, values are given as mean ± SEM of three independent experiments. *, $P < 0.05$; **, $P < 0.01$ versus *WT* (ANOVA).

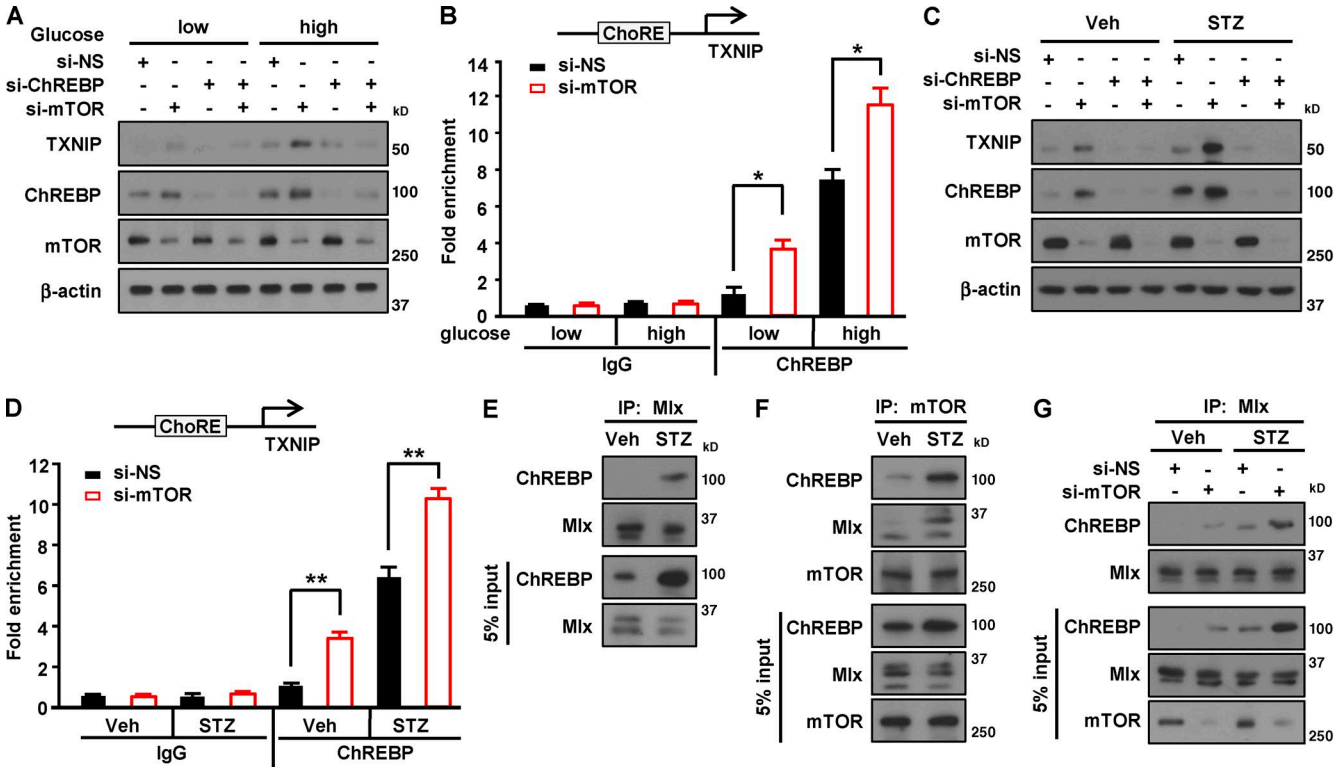

Figure 6. **mTOR interacts with the ChREBP–Mlx complex to inhibit its binding to TXNIP promoter.** (A) Expression of TXNIP and ChREBP after mTOR knockdown after high-glucose treatment. (B) Binding affinity of ChREBP to TXNIP promoter in INS-1 cells transfected with si-NS or si-mTOR upon high-glucose treatment. (C) Expression of TXNIP and ChREBP after mTOR knockdown under STZ treatment. (D) Binding of ChREBP to the ChoRE region of TXNIP promoter in INS-1 cells transfected with si-NS or si-mTOR after STZ treatment. (E) Interaction between Mlx and ChREBP in INS-1 cells upon STZ treatment. INS-1 cells were incubated with 1 mM STZ for 2 h. (F) Binding between mTOR and ChREBP or Mlx in INS-1 cells after STZ exposure. (G) Interaction between ChREBP and Mlx in INS-1 cells after STZ treatment. In B and D, values are given as mean ± SEM of three independent experiments. *, $P < 0.05$; **, $P < 0.01$ versus si-NS (ANOVA). IP, immunoprecipitate; Veh, vehicle.

(Fig. 7, D and E), indicating that diabetes-induced enhancement of TXNIP and ChREBP expression is conserved between mice and humans. Collectively, these results suggest that depletion of mTOR facilitates the association of ChREBP with Mlx and induces recruitment of the ChREBP–Mlx complex into the nucleus, where it binds the ChoRE region of the TXNIP promoter, thereby enhancing transcription of the TXNIP gene (Fig. 7 F).

Discussion

Insulin secretory function and survival of pancreatic β cells are intimately linked to nutrient availability and its sensing (Efeyan et al., 2015). Here, we report that mice lacking mTOR, a common nutrient-sensing component of mTORC1 and mTORC2, in β cells exhibited glucose intolerance, insulin resistance, a decrease in β cell mass, and an increase in β cell death. These results suggest that impaired glucose homeostasis is connected to a defect in β cell survival caused by mTOR deficiency. On the other hand, TSC2 deficiency in β cells, which leads to constitutive activation of mTORC1 signaling, results in a decrease in blood glucose levels, hyperinsulinemia, and improved glucose tolerance, which is the opposite phenotype of *mTOR*-deficient mice (Rachdi et al., 2008). Conversely, rapamycin and other mTORC1 inhibitors such as sirolimus, everolimus, and zatarolimus have been used to treat chronic diseases like cancer, hyperinsulinism, tuberous sclerosis complex, and lymphangioleiomyomatosis (Li et al., 2014). Considering that mTORC1 is critical for nutrient sensing (Jewell and Guan, 2013), it should be concerning that the long-term treatment of chronic diseases with mTORC1 inhibitors leads to adverse effects, including severe weight loss, hypertriglycemia, hypercholesterolemia, nephrotoxicity, altered insulin sensitivity, and immunodeficiency (Li et al., 2014). In β cells, rapamycin induces apoptosis in mouse and human islets, as well as in MIN6 cells upon chronic glucose exposure (Bell et al., 2003; Fraenkel et al., 2008). Our results and those of others suggest the relevance of mTOR signaling in β cell growth and survival in response to nutritional status and indicate the importance of determining the mechanism of the action of mTOR protein in controlling β cell survival and function.

Although it is well known that insulin resistance is commonly defined by inadequate response to insulin in peripheral tissues such as muscle, liver, and adipose tissue (Le Bacquer et al., 2007; Muoio and Newgard, 2008), we observed insulin resistance in β cell–specific *mTOR*-deficient mice. In patients with type 1 or type 2 diabetes, there are common cases of insulin resistance accompanied by a decrease in β cell mass and insulin secretion (Muoio and Newgard, 2008). It is possible that the phenotype of insulin resistance in *mTOR*-deficient mice may be connected to the markedly reduced in β cell mass and insulin secretion caused by mTOR deficiency. Given that β cells themselves are capable of producing chemokines and cytokines such as IL-1β, IFNγ, pancreatic-derived factor (PANDER), amylin, and apolipoprotein CIII in response to hyperglycemia (Cieślak et al., 2015), and considering that these chemokines

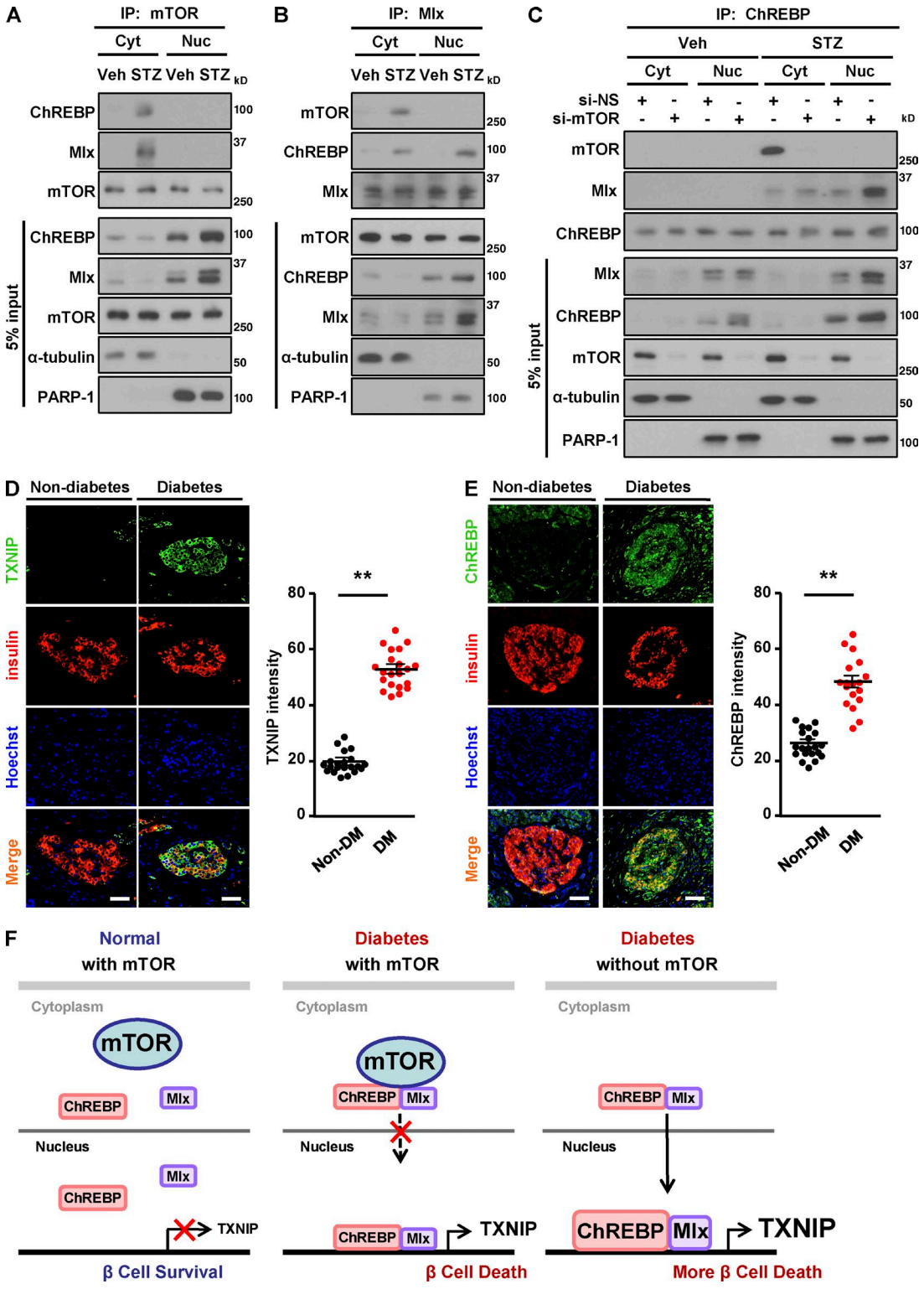

Figure 7. **Increased expression levels of TXNIP and ChREBP in human diabetic islets.** (A) Formation of ChREBP–Mlx complex after STZ treatment. (B) Translocation of the ChREBP–Mlx complex from the cytoplasm into the nucleus after STZ treatment. (C) Recruitment of the ChREBP–Mlx complex into the nucleus by mTOR knockdown after STZ treatment. (D) Increased expression levels of TXNIP in islets of nondiabetic and diabetic patients. (left) Representative pancreatic sections of nondiabetic control subjects and subjects with diabetes stained for TXNIP (green) and insulin (red). (right) Quantification of mean TXNIP intensity. (E) Enhanced expression levels of ChREBP in islets of diabetic patients. (left) Representative immunofluorescence images of human pancreatic sections from nondiabetic control subjects and subjects with diabetes using antibodies against ChREBP (green) and insulin (red). (right) Quantification of mean ChREBP intensity. (F) Proposed model of how mTOR regulates TXNIP expression and β cell survival in diabetic conditions. mTOR associates with the ChREBP–Mlx complex to inhibit its translocation into nucleus, blocking transcriptional activity, leading to the decrease in TXNIP transcription, and thereby protecting β cell survival upon STZ treatment. In D and E, nuclei are shown with Hoechst (blue) staining. Bars, 75 µm; non–diabetes mellitus (non-DM), n = 22 sections from 10 subjects; diabetes mellitus (DM), n = 16 sections from 7 subjects. Values are given as mean ± SEM. **, $P < 0.01$ versus non–diabetes mellitus (ANOVA). Cyt, cytoplasm; Nuc, nucleus; Veh, vehicle.

and cytokines contribute to insulin resistance and inflammation (Eizirik et al., 2009), it is possible that *mTOR*-deficient β cells might produce such secretory factors, which would affect insulin sensitivity in peripheral tissues. Identification of the kinds of secretory factors that are directly involved in insulin resistance in β cell–specific *mTOR*-deficient mice would be of interest, as it would likely identify the link between β cell dysfunction and insulin resistance in peripheral tissues.

Although it has been reported that RIP-Cre is expressed in the hypothalamic region (Kubota et al., 2004), we could not detect mTOR depletion in the hypothalamus. Notably, isolated *βmTORKO* islets exhibited increased expression of apoptotic proteins and a reduction in glucose-stimulated insulin secretion ex vivo, suggesting that the phenotype of *βmTORKO* mice is likely to be the consequence of mTOR deficiency specifically in β cells. Although the roles of S6K1, Akt, 4EBPs, raptor, and rictor in various cells and tissues, including β cells, have been investigated extensively (Bernal-Mizrachi et al., 2004; Le Bacquer et al., 2007; Bentzinger et al., 2008; Gu et al., 2011; Um et al., 2015), the function of mTOR in β cells remains to be determined. In this context, our analysis further revealed that mTOR deficiency resulted in decreased mitochondrial membrane potential and an increased ADP/ATP ratio, ultimately leading to reduced insulin secretion. Consistent with this, rapamycin inhibits glucose-stimulated insulin secretion in pancreatic islets by reducing mitochondrial ATP production through suppressing carbohydrate metabolism in the Krebs cycle (Shimodahira et al., 2010). Conversely, the ablation of TSC2 in β cells enhances insulin secretion by increasing the number of mitochondria via activation of mTORC1 (Koyanagi et al., 2011). However, it is unclear whether mitochondrial ATP synthetic capacity in β cells is also regulated by mTORC2 (Gu et al., 2011). Previous studies with rapamycin treatment suggest that multiple targets such as raptor, 4EBPs, and S6Ks are involved in β cell death and decreased insulin secretion, whereas our data using β cell–specific mTOR knockout mice indicate that mTOR acts as a critical regulator to protect β cell survival and function.

Considering that the prevalence of diabetes has been rising in recent decades (Kharroubi and Darwish, 2015), elucidation of the mechanisms by which nutrient-sensitive signaling regulates β cell survival and function is critical for developing novel therapeutic strategies for diabetes treatment. Here, we found that in the STZ-induced diabetic condition, β cell–specific *mTOR*-deficient mice exhibited severe glucose intolerance, impaired insulin secretion, markedly reduced islet size, and enhanced β cell death, suggesting a novel role of β cell–specific mTOR in the maintenance of glucose homeostasis in diabetes. Conversely, earlier studies have shown that mice expressing constitutively active Akt1 in β cells exhibit resistance to STZ-induced diabetes, although its effect on β cell survival and its molecular target have not been directly determined (Bernal-Mizrachi et al., 2001). Under diabetic conditions, high levels of oxidative stress directly inhibit mitochondrial ATP production and suppress insulin release in β cells (Yano et al., 2011). Oxidative stress is regulated by TXNIP, an endogenous inhibitor of thioredoxin (Lerner et al., 2012; Oslowski et al., 2012; Jung et al., 2013; Shalev, 2014). *mTOR*-deficient mice exhibited an increase in TXNIP expression and a reduction of Trx-1 expression, along with an increase in β cell apoptosis upon STZ treatment. On the other hand, overexpression of mTOR conversed the expression patterns of apoptotic-related proteins observed in mTOR-depleted cells, suggesting the role of mTOR in the regulation of the TXNIP–Trx-1 axis. Considering that TXNIP can also be considered as a suppressor of glucose uptake, which is independent of its function as a regulator of oxidative stress via interacting with Trx (Patwari et al., 2009), it is critical to dissect the involvement of TXNIP as a suppressor of glucose uptake in the regulation of β cell function in the future using TXNIP C247S mutant construct, which leads to the loss of interaction of TXNIP with Trx and does not affect to the inhibitory function of TXNIP on glucose uptake (Patwari et al., 2009).

To date, the molecular mechanism that leads to increased TXNIP expression in diabetes is not fully defined. In this context, we found that mTOR acts as an inhibitory signaling component to control ChREBP-regulated TXNIP transcription in β cells. Considering that elevated TXNIP levels induce β cell oxidative stress and apoptosis (Lerner et al., 2012; Oslowski et al., 2012), whereas deficiency of TXNIP protects against type 1 diabetes by inducing β cell survival (Chen et al., 2008), the capacity of mTOR to suppress ChREBP-mediated TXNIP expression may play a crucial role in protecting β cells from death in diabetes. In line with this, Kaadige et al. (2015) have recently reported that mTOR negatively regulates TXNIP expression in HEK 293T cells. Their study described the relationship between TXNIP–mTOR and Mondo A (Kaadige et al., 2015), which is known to be primarily expressed in muscle and heart but lacks two essential cAMP-dependent protein kinase phosphorylation sites important for glucose responsiveness (Li et al., 2006). Our analysis showed that in β cells, mTOR binds to the ChREBP–Mlx complex, which is critical to glucose responsiveness. Mechanistically, we found that mTOR inhibits translocation of this complex into the nucleus, suppressing ChREBP transcriptional activity required for TXNIP expression in β cells. Although ChREBP is not Mondo A, and we used primary pancreatic β cells, whereas Kaadige et al. (2015) used HEK293T and BxPC-3 cell lines, our study further expends their findings to the levels of β cell physiology in vivo and pathological human relevance in the regard of mTOR-mediated TXNIP expression (Kaadige et al., 2015). Consistent with the study by Kaadige et al. (2015), our analysis further indicated that raptor, rather than rictor, was mainly involved in mTOR-regulated TXNIP expression. However, our data do not completely rule out the possibility that mTORC2 may regulate TXNIP expression or its association with Mlx. It will be important to determine whether the roles of mTOR on β cell survival and function are mediated through mTORC1 or mTORC2 in vivo. This might be addressed by analysis of β cell–specific *raptor*-deficient mice or β cell–specific *rictor*-deficient mice under diabetic conditions. Considering the elevated expression of TXNIP and ChREBP in *mTOR*-deficient mice, whether the involvement of *TXNIP* and *ChREBP* expression is correlated with observed phenotypes should be directly tested in TXNIP- or ChREBP-deficient mice or knockdown cells in the future.

The clinical significance of our findings was illustrated by the results showing that expression levels of TXNIP and ChREBP were elevated in human diabetic islets, which was consistent with the loss of glycemic control. Considering that rapamycin, an immunosuppressant, causes a large population of transplanted islets to undergo apoptosis accompanied by a deterioration of glucose homeostasis (Barlow et al., 2013), rapamycin-mediated inhibition of mTORC1 activity may render islet β cells more susceptible to oxidative stress and β cell dysfunction during transplantation. Indeed, a high incidence of hyperglycemia and development of new-onset diabetes has been reported

in 13–50% of patients in clinical trials using mTOR inhibitors as anticancer therapies (Vergès and Cariou, 2015). Thus, our findings suggest that controlling the nutrient-sensitive mTOR-regulated transcriptional network may provide a means to preserve β cell survival and function in diabetes or islet grafts.

Materials and methods

Mice

mTOR$^{flox/flox}$ and *Rip-Cre* mice were purchased from The Jackson Laboratory. All mice were backcrossed 10 times onto the C57BL/6J background maintained on a 12-h light/dark cycle and fed ad libitum. All animal experiments were approved by the Institutional Animal Care and Use Committee of Sungkyunkwan University School of Medicine. Sungkyunkwan University School of Medicine is an Association for Assessment and Accreditation of Laboratory Animal Care International–accredited facility and abides by the Institute of Laboratory Animal Resources guide.

Human pancreas sections

Human pancreas sections were obtained from pancreata of nondiabetic and diabetic subjects under approval of the Health Research Ethics Board of Seoul National University Hospital and after obtaining informed consent (26–2016-109). Human pancreas sections were obtained from 10 nondiabetic adult subjects (mean age, 53.17 ± 3 yr [range, 38–79 yr]; body mass index, 22.04 ± 0.65 (range, 17.8–29.4 kg/m^2), and from 7 diabetic subjects: mean age, 53.17 ± 3 yr (range, 38–79 yr); body mass index, 22.04 ± 0.65 (range, 17.8–29.4 kg/m^2); HbA1c in diabetic subjects, 7.14 ± 1.02%. Pancreas sections were costained with ChREBP and insulin, or with TXNIP and insulin antibodies. Subject details are presented in Table S1.

Cell culture and transfection

Rat insulinoma (INS-1) cells were provided by C. Newgard (Duke University, Durham, NC) and grown as previously described (Oslowski et al., 2012). INS-1 cells were transfected with 10 nM siRNA using DharmaFECT1 transfection reagent (GE Healthcare). The sense and antisense sequences of siRNAs were as follows: nonsilencing, 5′-UUCUCCGAACGUGUCACGUUU-3′ and 5′-ACGUGACACGUUCGGAGAAUU-3′; mTOR, 5′-GGCCUAUGGUCGAGAUUUAUU-3′ and 5′-UAAAUCUCGACCAUAGGCCUU-3′; ChREBP #1, 5′-AAGAGGCGUUUCAAUAUUAUU-3′ and 5′-UAAUAUUGAAACGCCUCUUUU-3′; and ChREBP #2, 5′-GCAACUGAGGGAUGAAAUAUU-3′ and 5′-UAUUUCAUCCCUCAGUUGCUU-3′. siRNAs against raptor or rictor were purchased from Santa Cruz Biotechnology, Inc. For overexpressing of mTOR, INS-1 cells were transfected with indicated pRK5-based expression vectors: myc-mTOR (Addgene) and myc-mTOR kinase dead (myc-mTOR KD; Addgene). The total amount of plasmid DNA in each transfection was normalized with empty pRK5.

Immunoblotting and immunoprecipitation

Cells were lysed in a radioimmunoprecipitation assay buffer containing 150 mM NaCl, 50 mM Tris-Cl, pH 7.4, 1 mM EDTA, 1% NP-40, 0.25% sodium-deoxycholate, 0.1 M NaF, 2 mM Na_3VO_4, and protease inhibitors (Roche). The process of immunoblotting and immunoprecipitation was performed as previously described (Kim et al., 2012). Antibodies against mTOR (rabbit), raptor (rabbit), rictor (rabbit), PARP (rabbit), p-S6 S235/236 (rabbit), p-S6 S240/244 (rabbit), p-Akt S473 (rabbit), and p-S6K T389 (rabbit) were purchased from Cell Signaling Technology. Antibodies against TXNIP (mouse), ChREBP (goat), Mlx (goat), Bax (mouse), Bcl-2 (mouse), α-tubulin (mouse), and β actin (goat) were purchased from Santa Cruz Biotechnology, Inc. Anti–Trx-1 antibody (mouse) was obtained from BD. All immunoblotting and immunoprecipitation experiments were performed independently at least three times.

Glucose tolerance test, insulin tolerance test, and measurement of serum insulin levels

For the glucose tolerance test, mice were fasted for 16 h and then injected i.p. with D-glucose (2 g/kg body weight) in sterile PBS. For the insulin tolerance test, mice were fasted for 4 h and then injected i.p. with insulin (0.75 U/kg body weight). Blood glucose levels were measured at 0, 15, 30, 60, 90, and 120 min using an AccuChek II glucometer (Roche) after challenge with glucose or insulin. To measure serum insulin levels, blood was collected from the tail vein before and 15 and 30 min after intraperitoneal injection with glucose (2 g/kg body weight). Blood samples were centrifuged, and serum was collected for the measurement of insulin concentrations with an ELISA Mouse Insulin kit (ALPCO).

Islet isolation

Islets were isolated from 8-wk-old male mice as described previously (Um et al., 2015). In brief, mouse pancreata were injected with 0.8 mg/ml collagenase P (Roche) in HBSS solution. The entire pancreas was incubated at 37°C for 15 min with regular shaking. The digested suspension was passed through a mesh (Sigma-Aldrich), and islets were isolated by density gradient centrifugation on a Ficoll gradient (Biochrom AG). After centrifugation without braking, islets were collected from the interface and hand-picked into a Petri dish under a dissecting microscope. Isolated islets were cultured at 37°C in RPMI 1640 with 10% FBS and 1% penicillin/streptomycin overnight under humidified conditions of 95% air and 5% CO_2 before performing the experimental procedures.

Immunohistochemistry

Pancreata obtained from 12-wk-old mice were used for morphometric analysis and immunohistochemistry. Immunostaining for insulin (guinea pig; Dako; or rabbit; Santa Cruz Biotechnology, Inc.), glucagon (mouse; Sigma-Aldrich), and Ki67 (mouse; Santa Cruz Biotechnology, Inc.), TXNIP (mouse; MBL), ChREBP (goat; Santa Cruz Biotechnology, Inc.), p-S6 S235/236 (rabbit; Cell Signaling Technology), p-mTOR S2448 (rabbit; Cell Signaling Technology) was performed as previously described (Um et al., 2015). Immunostaining was performed in slides with pancreas, presenting 1/6 of the organ. Slides incubated with primary antibodies were visualized with Alexa Fluor 568– or 488–conjugated IgG (Invitrogen) by fluorescence microscopy (Axiovert-200; ZEISS). Mean islet volume and β cell density were measured in insulin- and glucagon-stained pancreas sections using ImageJ software (National Institutes of Health). β Cell mass was determined using the following equation: β cell mass = pancreas weight (milligrams) × relative insulin surface (total area of insulin-positive cells [square micrometers]/total pancreas area [square micrometers]) × 100 (Um et al., 2015).

Assay of insulin secretion from isolated islets and INS-1 cells

To assay insulin release in islets, groups of 10 islets in triplicate were preincubated and then stimulated with either 2.8 mM or 16.7 mM glucose in Krebs-Ringer buffer (135 mM NaCl, 3.6 mM KCl, 0.5 mM NaH_2PO_4, 0.5 mM $MgSO_4$,1.5 mM $CaCl_2$, 5 mM $NaHCO_3$, 10 mM Hepes, and 0.1% BSA, pH 7.4). For insulin content measurement, islets were incubated overnight in acidic ethanol solution (75% ethanol and 25% CH_3COOH) and then sonicated on ice (Sonic Dismembrator 500; Thermo Fisher Scientific). After centrifugation, supernatants

were collected for measurement of insulin content using ELISA kit (ALPCO). To assay insulin secretion in INS-1 cells, 3 d after transfection, cells were preincubated for 1 h in Krebs-Ringer buffer containing 3 mM glucose at 37°C. Thereafter, cells were incubated with Krebs-Ringer buffer containing 3 mM or 25 mM glucose for another 1 h at 37°C. The supernatants were collected for measurement of insulin secretion using an ELISA kit (ALPCO).

Chromatin immunoprecipitation assay

INS-1 cells were seeded onto 10-cm dishes in RPMI-1640 medium 1 d before the treatment. The cells were incubated in RPMI-1640 containing 5 mM or 25 mM glucose for 6 h. Cells were cross-linked with 1% formaldehyde for 10 min. Glycine was added at a final concentration of 0.125 M to terminate the cross-linking reaction. Cells were washed with PBS, suspended in SDS lysis buffer, and then subjected to sonication with a Sonic Dismembrator 500 (Thermo Fisher Scientific). DNA–protein complexes were immunoprecipitated for 16 h at 4°C with anti-ChREBP. Protein and/or DNA complexes were captured for 1 h at 4°C using protein A or G agarose (GE Healthcare)/salmon sperm DNA slurry and extensively washed. The cross-links were reversed by heating to 65°C for 4 h in Tris-HCl, pH 6.5, 5 M NaCl, and 0.5 M EDTA. DNA was extracted by phenol/$CHCl_3$ and precipitated with ethanol. Precipitated DNA was quantified by quantitative PCR with the following primers: rat TXNIP, 5′-CGCACCCGAACAACAACCAT-3′ (forward), 3′-AAGCGGGAGCCGGAAACGG-5′ (reverse); rat GAPDH, 5′-ACCATGCTTCACTGACATTCTGA-3′ (forward), 3′-GGTCTGCCTCCCTGCTAACC-5′ (reverse).

$[Ca^{2+}]_i$ measurement

Ca^{2+} measurement was performed as previously described with modifications (Phuong et al., 2013). Pancreatic islets were incubated in culture medium containing 4 µM fura 2-AM for 30 min at room temperature. Islets were washed twice with Tyrode solution (in millimoles per liter, 145 NaCl, 5 KCl, 1.5 $CaCl_2$, 3 glucose, and 10 Hepes, pH 7.4, with NaOH) and placed in the dark for 30 min. Islets were placed into a recording chamber and alternatively excited (340 and 380 nm) at 5 Hz frequency, and the emitted fluorescence at 510 nm was collected via a photomultiplier tube (PTI). A mechanical diaphragm situated at an image plane in the emission path limited the measurement to a single islet. The measurement was performed at 36°C, and the islets were alternatively superfused (~3 ml/min) with Tyrode solution containing 3 mM or 16.7 mM glucose or 60 mM KCl. The fluorescence ratios (F_{340}/F_{380}) were recorded using Felix32 (PTI). The data were analyzed using Origin 6.1 software.

Cell cycle analysis

3 d after transfection with either control siRNA (si-NS) or mTOR siRNA (si-mTOR), INS-1 cells were treated with 1 mM STZ for 24 h. The cells were trypsinized, washed twice with PBS, and fixed with 70% ice-cold ethanol. Cells were washed with cold PBS and incubated with 0.2 mg/ml RNase A (Sigma-Aldrich) at 37°C for 30 min. Finally, cells were labeled with propidium iodide at final concentration 20 µg/ml (Sigma-Aldrich) for 30 min in the dark at room temperature and processed further by flow cytometry using a Canto II cell sorter (BD). The populations of cells in sub-G2/M, S, G1, and sub-G1 phase were gated and analyzed using FACS BD Canto II software.

Measurement of intracellular ROS production and mitochondrial membrane potential

For measurement of intracellular ROS levels, cells were washed twice with PBS and incubated in PBS containing 10 µM fluorescence probe 2′,7′-dichlorofluorescein diacetate (Invitrogen) for 30 min in the dark at 37°C. Mitochondrial membrane potential was assessed by staining cells with 10 nM tetramethylrhodamine, ethyl ester (Invitrogen) for 30 min in the dark at 37°C. Intracellular ROS levels and mitochondrial membrane potentials were quantified by flow cytometry using a Canto II cell sorter.

Measurement of mitochondrial respiration

The oxygen consumption rate of isolated islets was measured using a Seahorse XF24 extracellular flux analyzer according to the manufacturer's instructions. In brief, 20 mM glucose was added to stimulate cellular oxygen consumption. 5 µM oligomycin, 1 µM FCCP, or 5 µM rotenone was added at indicated times.

Statistical analysis

Data are presented as mean ± SEM. All experiments were repeated at least three times, with representative data shown. The main and interactive effects were analyzed by ANOVA factorial or repeated measurements or by one-way ANOVA. Differences between individual group means were analyzed by post hoc Bonferroni test or two-tailed *t* test. Analyses were performed using GraphPad Prism software. Differences were considered to be statistically significant at $P < 0.05$.

Online supplemental material

Fig. S1 shows the genotyping and body weight of mice used in this study. Fig. S2 shows that the depletion of mTOR or inhibition of mTOR activity results in increased TXNIP and ChREBP expression. Table S1 shows information regarding human islets.

Acknowledgments

We thank Drs. George Thomas, Sara Kozma, and Young-Hoon Jang for helpful discussions and Dr. Thi Thanh Tam Phuong for $[Ca^{2+}]_i$ measurement.

This study was supported by the National Research Foundation of Korea (grants 2014R1A2A1A11050734 and 2016R1A4A1011189) and the Korea Healthcare Technology Research and Development Project, Ministry for Health, Welfare, and Family Affairs, Korea (grant HI14C0336).

The authors declare no competing financial interests.

Author contributions: G.C. Chau, D.U. Im, and S.H. Um conceived the project and designed experiments. G.C. Chau, D.U. Im, and T.M. Kang performed the experiments. G.C. Chau, D.U. Im, T.M. Kang, J.M. Bae, W. Kim, E.-Y. Moon, S. Pyo, and S.H. Um analyzed data. G.C. Chau and S.H. Um wrote and edited the manuscript.

Submitted: 17 January 2017
Revised: 5 April 2017
Accepted: 1 May 2017

References

Alejandro, E.U., B. Gregg, T. Wallen, D. Kumusoglu, D. Meister, A. Chen, M.J. Merrins, L.S. Satin, M. Liu, P. Arvan, and E. Bernal-Mizrachi. 2014. Maternal diet-induced microRNAs and mTOR underlie β cell dysfunction in offspring. *J. Clin. Invest.* 124:4395–4410. http://dx.doi.org/10.1172/JCI74237

Barlow, A.D., M.L. Nicholson, and T.P. Herbert. 2013. Evidence for rapamycin toxicity in pancreatic β-cells and a review of the underlying molecular mechanisms. *Diabetes.* 62:2674–2682. http://dx.doi.org/10.2337/db13-0106

Bar-Peled, L., L.D. Schweitzer, R. Zoncu, and D.M. Sabatini. 2012. Ragulator is a GEF for the rag GTPases that signal amino acid levels to mTORC1. *Cell.* 150:1196–1208. http://dx.doi.org/10.1016/j.cell.2012.07.032

Bar-Peled, L., L. Chantranupong, A.D. Cherniack, W.W. Chen, K.A. Ottina, B.C. Grabiner, E.D. Spear, S.L. Carter, M. Meyerson, and D.M. Sabatini. 2013. A Tumor suppressor complex with GAP activity for the Rag

GTPases that signal amino acid sufficiency to mTORC1. *Science.* 340:1100–1106. http://dx.doi.org/10.1126/science.1232044

Bell, E., X. Cao, J.A. Moibi, S.R. Greene, R. Young, M. Trucco, Z. Gao, F.M. Matschinsky, S. Deng, J.F. Markman, et al. 2003. Rapamycin has a deleterious effect on MIN-6 cells and rat and human islets. *Diabetes.* 52:2731–2739. http://dx.doi.org/10.2337/diabetes.52.11.2731

Bentzinger, C.F., K. Romanino, D. Cloëtta, S. Lin, J.B. Mascarenhas, F. Oliveri, J. Xia, E. Casanova, C.F. Costa, M. Brink, et al. 2008. Skeletal muscle-specific ablation of raptor, but not of rictor, causes metabolic changes and results in muscle dystrophy. *Cell Metab.* 8:411–424. http://dx.doi.org/10.1016/j.cmet.2008.10.002

Bernal-Mizrachi, E., W. Wen, S. Stahlhut, C.M. Welling, and M.A. Permutt. 2001. Islet β cell expression of constitutively active Akt1/PKB α induces striking hypertrophy, hyperplasia, and hyperinsulinemia. *J. Clin. Invest.* 108:1631–1638. http://dx.doi.org/10.1172/JCI200113785

Bernal-Mizrachi, E., S. Fatrai, J.D. Johnson, M. Ohsugi, K. Otani, Z. Han, K.S. Polonsky, and M.A. Permutt. 2004. Defective insulin secretion and increased susceptibility to experimental diabetes are induced by reduced Akt activity in pancreatic islet β cells. *J. Clin. Invest.* 114:928–936. http://dx.doi.org/10.1172/JCI200420016

Butler, A.E., J. Janson, S. Bonner-Weir, R. Ritzel, R.A. Rizza, and P.C. Butler. 2003. β-cell deficit and increased β-cell apoptosis in humans with type 2 diabetes. *Diabetes.* 52:102–110. http://dx.doi.org/10.2337/diabetes.52.1.102

Cha-Molstad, H., G. Saxena, J. Chen, and A. Shalev. 2009. Glucose-stimulated expression of Txnip is mediated by carbohydrate response element-binding protein, p300, and histone H4 acetylation in pancreatic β cells. *J. Biol. Chem.* 284:16898–16905. http://dx.doi.org/10.1074/jbc.M109.010504

Chantranupong, L., S.M. Scaria, R.A. Saxton, M.P. Gygi, K. Shen, G.A. Wyant, T. Wang, J.W. Harper, S.P. Gygi, and D.M. Sabatini. 2016. The CASTOR proteins are arginine sensors for the mTORC1 pathway. *Cell.* 165:153–164. http://dx.doi.org/10.1016/j.cell.2016.02.035

Chen, J., S.T. Hui, F.M. Couto, I.N. Mungrue, D.B. Davis, A.D. Attie, A.J. Lusis, R.A. Davis, and A. Shalev. 2008. Thioredoxin-interacting protein deficiency induces Akt/Bcl-xL signaling and pancreatic β-cell mass and protects against diabetes. *FASEB J.* 22:3581–3594. http://dx.doi.org/10.1096/fj.08-111690

Cieślak, M., A. Wojtczak, and M. Cieślak. 2015. Role of pro-inflammatory cytokines of pancreatic islets and prospects of elaboration of new methods for the diabetes treatment. *Acta Biochim. Pol.* 62:15–21. http://dx.doi.org/10.18388/abp.2014_853

Ebato, C., T. Uchida, M. Arakawa, M. Komatsu, T. Ueno, K. Komiya, K. Azuma, T. Hirose, K. Tanaka, E. Kominami, et al. 2008. Autophagy is important in islet homeostasis and compensatory increase of β cell mass in response to high-fat diet. *Cell Metab.* 8:325–332. http://dx.doi.org/10.1016/j.cmet.2008.08.009

Efeyan, A., W.C. Comb, and D.M. Sabatini. 2015. Nutrient-sensing mechanisms and pathways. *Nature.* 517:302–310. http://dx.doi.org/10.1038/nature14190

Eizirik, D.L., M.L. Colli, and F. Ortis. 2009. The role of inflammation in insulitis and β-cell loss in type 1 diabetes. *Nat. Rev. Endocrinol.* 5:219–226. http://dx.doi.org/10.1038/nrendo.2009.21

Fraenkel, M., M. Ketzinel-Gilad, Y. Ariav, O. Pappo, M. Karaca, J. Castel, M.-F. Berthault, C. Magnan, E. Cerasi, N. Kaiser, and G. Leibowitz. 2008. mTOR inhibition by rapamycin prevents β-cell adaptation to hyperglycemia and exacerbates the metabolic state in type 2 diabetes. *Diabetes.* 57:945–957. http://dx.doi.org/10.2337/db07-0922

Gangloff, Y.G., M. Mueller, S.G. Dann, P. Svoboda, M. Sticker, J.F. Spetz, S.H. Um, E.J. Brown, S. Cereghini, G. Thomas, and S.C. Kozma. 2004. Disruption of the mouse mTOR gene leads to early postimplantation lethality and prohibits embryonic stem cell development. *Mol. Cell. Biol.* 24:9508–9516. http://dx.doi.org/10.1128/MCB.24.21.9508-9516.2004

Gleason, C.E., D. Lu, L.A. Witters, C.B. Newgard, and M.J. Birnbaum. 2007. The role of AMPK and mTOR in nutrient sensing in pancreatic β-cells. *J. Biol. Chem.* 282:10341–10351. http://dx.doi.org/10.1074/jbc.M610631200

Gu, Y., J. Lindner, A. Kumar, W. Yuan, and M.A. Magnuson. 2011. Rictor/mTORC2 is essential for maintaining a balance between β-cell proliferation and cell size. *Diabetes.* 60:827–837. http://dx.doi.org/10.2337/db10-1194

Halban, P.A., K.S. Polonsky, D.W. Bowden, M.A. Hawkins, C. Ling, K.J. Mather, A.C. Powers, C.J. Rhodes, L. Sussel, and G.C. Weir. 2014. β-cell failure in type 2 diabetes: postulated mechanisms and prospects for prevention and treatment. *J. Clin. Endocrinol. Metab.* 99:1983–1992. http://dx.doi.org/10.1210/jc.2014-1425

Han, J.M., S.J. Jeong, M.C. Park, G. Kim, N.H. Kwon, H.K. Kim, S.H. Ha, S.H. Ryu, and S. Kim. 2012. Leucyl-tRNA synthetase is an intracellular leucine sensor for the mTORC1-signaling pathway. *Cell.* 149:410–424. http://dx.doi.org/10.1016/j.cell.2012.02.044

Heit, J.J., S.K. Karnik, and S.K. Kim. 2006. Intrinsic regulators of pancreatic β-cell proliferation. *Annu. Rev. Cell Dev. Biol.* 22:311–338. http://dx.doi.org/10.1146/annurev.cellbio.22.010305.104425

Henquin, J.C. 2000. Triggering and amplifying pathways of regulation of insulin secretion by glucose. *Diabetes.* 49:1751–1760. http://dx.doi.org/10.2337/diabetes.49.11.1751

Houde, V.P., S. Brûlé, W.T. Festuccia, P.-G. Blanchard, K. Bellmann, Y. Deshaies, and A. Marette. 2010. Chronic rapamycin treatment causes glucose intolerance and hyperlipidemia by upregulating hepatic gluconeogenesis and impairing lipid deposition in adipose tissue. *Diabetes.* 59:1338–1348. http://dx.doi.org/10.2337/db09-1324

Huh, K.H., Y. Cho, B.S. Kim, J.H. Do, Y.J. Park, D.J. Joo, M.S. Kim, and Y.S. Kim. 2013. The role of thioredoxin 1 in the mycophenolic acid-induced apoptosis of insulin-producing cells. *Cell Death Dis.* 4:e721. http://dx.doi.org/10.1038/cddis.2013.247

Jewell, J.L., and K.-L. Guan. 2013. Nutrient signaling to mTOR and cell growth. *Trends Biochem. Sci.* 38:233–242. http://dx.doi.org/10.1016/j.tibs.2013.01.004

Jung, H.S., K.W. Chung, J. Won Kim, J. Kim, M. Komatsu, K. Tanaka, Y.H. Nguyen, T.M. Kang, K.-H. Yoon, J.-W. Kim, et al. 2008. Loss of autophagy diminishes pancreatic β cell mass and function with resultant hyperglycemia. *Cell Metab.* 8:318–324. http://dx.doi.org/10.1016/j.cmet.2008.08.013

Jung, H., M.J. Kim, D.O. Kim, W.S. Kim, S.J. Yoon, Y.J. Park, S.R. Yoon, T.D. Kim, H.W. Suh, S. Yun, et al. 2013. TXNIP maintains the hematopoietic cell pool by switching the function of p53 under oxidative stress. *Cell Metab.* 18:75–85. http://dx.doi.org/10.1016/j.cmet.2013.06.002

Kaadige, M.R., J. Yang, B.R. Wilde, and D.E. Ayer. 2015. MondoA-Mlx transcriptional activity is limited by mTOR-MondoA interaction. *Mol. Cell. Biol.* 35:101–110. http://dx.doi.org/10.1128/MCB.00636-14

Kharroubi, A.T., and H.M. Darwish. 2015. Diabetes mellitus: The epidemic of the century. *World J. Diabetes.* 6:850–867. http://dx.doi.org/10.4239/wjd.v6.i6.850

Kibbe, C., J. Chen, G. Xu, G. Jing, and A. Shalev. 2013. FOXO1 competes with carbohydrate response element-binding protein (ChREBP) and inhibits thioredoxin-interacting protein (TXNIP) transcription in pancreatic β cells. *J. Biol. Chem.* 288:23194–23202. http://dx.doi.org/10.1074/jbc.M113.473082

Kim, K., S. Pyo, and S.H. Um. 2012. S6 kinase 2 deficiency enhances ketone body production and increases peroxisome proliferator-activated receptor α activity in the liver. *Hepatology.* 55:1727–1737. http://dx.doi.org/10.1002/hep.25537

Koyanagi, M., S. Asahara, T. Matsuda, N. Hashimoto, Y. Shigeyama, Y. Shibutani, A. Kanno, M. Fuchita, T. Mikami, T. Hosooka, et al. 2011. Ablation of TSC2 enhances insulin secretion by increasing the number of mitochondria through activation of mTORC1. *PLoS One.* 6:e23238. http://dx.doi.org/10.1371/journal.pone.0023238

Krause, M.S., N.H. McClenaghan, P.R. Flatt, P.I. de Bittencourt, C. Murphy, and P. Newsholme. 2011. L-arginine is essential for pancreatic β-cell functional integrity, metabolism and defense from inflammatory challenge. *J. Endocrinol.* 211:87–97. http://dx.doi.org/10.1530/JOE-11-0236

Kubota, N., Y. Terauchi, K. Tobe, W. Yano, R. Suzuki, K. Ueki, I. Takamoto, H. Satoh, T. Maki, T. Kubota, et al. 2004. Insulin receptor substrate 2 plays a crucial role in β cells and the hypothalamus. *J. Clin. Invest.* 114:917–927. http://dx.doi.org/10.1172/JCI21484

Laplante, M., and D.M. Sabatini. 2012. mTOR signaling in growth control and disease. *Cell.* 149:274–293. http://dx.doi.org/10.1016/j.cell.2012.03.017

Le Bacquer, O., E. Petroulakis, S. Paglialunga, F. Poulin, D. Richard, K. Cianflone, and N. Sonenberg. 2007. Elevated sensitivity to diet-induced obesity and insulin resistance in mice lacking 4E-BP1 and 4E-BP2. *J. Clin. Invest.* 117:387–396. http://dx.doi.org/10.1172/JCI29528

Lee, J.M., J.Y. Lim, Y. Kim, Y.J. Kim, H.S. Choi, E.S. Kim, B. Keum, Y.S. Seo, Y.T. Jeen, H.S. Lee, et al. 2016. Benexate hydrochloride betadex modulates nitric oxide synthesis and cytokine expression in gastric ulcers. *Exp. Ther. Med.* 12:573–580.

Lerner, A.G., J.P. Upton, P.V. Praveen, R. Ghosh, Y. Nakagawa, A. Igbaria, S. Shen, V. Nguyen, B.J. Backes, M. Heiman, et al. 2012. IRE1α induces thioredoxin-interacting protein to activate the NLRP3 inflammasome and promote programmed cell death under irremediable ER stress. *Cell Metab.* 16:250–264. http://dx.doi.org/10.1016/j.cmet.2012.07.007

Li, J., S.G. Kim, and J. Blenis. 2014. Rapamycin: One drug, many effects. *Cell Metab.* 19:373–379. http://dx.doi.org/10.1016/j.cmet.2014.01.001

Li, M.V., B. Chang, M. Imamura, N. Poungvarin, and L. Chan. 2006. Glucose-dependent transcriptional regulation by an evolutionarily conserved glucose-sensing module. *Diabetes.* 55:1179–1189. http://dx.doi.org/10.2337/db05-0822

Maechler, P. 2013. Mitochondrial function and insulin secretion. *Mol. Cell. Endocrinol.* 379:12–18. http://dx.doi.org/10.1016/j.mce.2013.06.019

Mori, H., K. Inoki, D. Opland, H. Münzberg, E.C. Villanueva, M. Faouzi, T. Ikenoue, D.J. Kwiatkowski, O.A. Macdougald, M.G. Myers Jr., and K.L. Guan. 2009. Critical roles for the TSC-mTOR pathway in β-cell function. *Am. J. Physiol. Endocrinol. Metab.* 297:E1013–E1022. http://dx.doi.org/10.1152/ajpendo.00262.2009

Muoio, D.M., and C.B. Newgard. 2008. Mechanisms of disease: Molecular and metabolic mechanisms of insulin resistance and β-cell failure in type 2 diabetes. *Nat. Rev. Mol. Cell Biol.* 9:193–205. http://dx.doi.org/10.1038/nrm2327

Murakami, M., T. Ichisaka, M. Maeda, N. Oshiro, K. Hara, F. Edenhofer, H. Kiyama, K. Yonezawa, and S. Yamanaka. 2004. mTOR is essential for growth and proliferation in early mouse embryos and embryonic stem cells. *Mol. Cell. Biol.* 24:6710–6718. http://dx.doi.org/10.1128/MCB.24.15.6710-6718.2004

Oslowski, C.M., T. Hara, B. O'Sullivan-Murphy, K. Kanekura, S. Lu, M. Hara, S. Ishigaki, L.J. Zhu, E. Hayashi, S.T. Hui, et al. 2012. Thioredoxin-interacting protein mediates ER stress-induced β cell death through initiation of the inflammasome. *Cell Metab.* 16:265–273. http://dx.doi.org/10.1016/j.cmet.2012.07.005

Patwari, P., W.A. Chutkow, K. Cummings, V.L.R.M. Verstraeten, J. Lammerding, E.R. Schreiter, and R.T. Lee. 2009. Thioredoxin-independent regulation of metabolism by the α-arrestin proteins. *J. Biol. Chem.* 284:24996–25003. http://dx.doi.org/10.1074/jbc.M109.018093

Pende, M., S.C. Kozma, M. Jaquet, V. Oorschot, R. Burcelin, Y. Le Marchand-Brustel, J. Klumperman, B. Thorens, and G. Thomas. 2000. Hypoinsulinaemia, glucose intolerance and diminished β-cell size in S6K1-deficient mice. *Nature.* 408:994–997. http://dx.doi.org/10.1038/35050135

Phuong, T.T.T., Y.-H. Yun, S.J. Kim, and T.M. Kang. 2013. Positive feedback control between STIM1 and NFATc3 is required for C2C12 myoblast differentiation. *Biochem. Biophys. Res. Commun.* 430:722–728. http://dx.doi.org/10.1016/j.bbrc.2012.11.082

Rachdi, L., N. Balcazar, F. Osorio-Duque, L. Elghazi, A. Weiss, A. Gould, K.J. Chang-Chen, M.J. Gambello, and E. Bernal-Mizrachi. 2008. Disruption of Tsc2 in pancreatic β cells induces β cell mass expansion and improved glucose tolerance in a TORC1-dependent manner. *Proc. Natl. Acad. Sci. USA.* 105:9250–9255. http://dx.doi.org/10.1073/pnas.0803047105

Russell, R.C., H.-X. Yuan, and K.-L. Guan. 2014. Autophagy regulation by nutrient signaling. *Cell Res.* 24:42–57. http://dx.doi.org/10.1038/cr.2013.166

Sakai, K., K. Matsumoto, T. Nishikawa, M. Suefuji, K. Nakamaru, Y. Hirashima, J. Kawashima, T. Shirotani, K. Ichinose, M. Brownlee, and E. Araki. 2003. Mitochondrial reactive oxygen species reduce insulin secretion by pancreatic β-cells. *Biochem. Biophys. Res. Commun.* 300:216–222. http://dx.doi.org/10.1016/S0006-291X(02)02832-2

Sancak, Y., T.R. Peterson, Y.D. Shaul, R.A. Lindquist, C.C. Thoreen, L. Bar-Peled, and D.M. Sabatini. 2008. The Rag GTPases bind raptor and mediate amino acid signaling to mTORC1. *Science.* 320:1496–1501. http://dx.doi.org/10.1126/science.1157535

Sancak, Y., L. Bar-Peled, R. Zoncu, A.L. Markhard, S. Nada, and D.M. Sabatini. 2010. Ragulator-Rag complex targets mTORC1 to the lysosomal surface and is necessary for its activation by amino acids. *Cell.* 141:290–303. http://dx.doi.org/10.1016/j.cell.2010.02.024

Shalev, A. 2014. Minireview: Thioredoxin-interacting protein: Regulation and function in the pancreatic β-cell. *Mol. Endocrinol.* 28:1211–1220. http://dx.doi.org/10.1210/me.2014-1095

Shimobayashi, M., and M.N. Hall. 2014. Making new contacts: The mTOR network in metabolism and signalling crosstalk. *Nat. Rev. Mol. Cell Biol.* 15:155–162. http://dx.doi.org/10.1038/nrm3757

Shimodahira, M., S. Fujimoto, E. Mukai, Y. Nakamura, Y. Nishi, M. Sasaki, Y. Sato, H. Sato, M. Hosokawa, K. Nagashima, et al. 2010. Rapamycin impairs metabolism-secretion coupling in rat pancreatic islets by suppressing carbohydrate metabolism. *J. Endocrinol.* 204:37–46. http://dx.doi.org/10.1677/JOE-09-0216

Um, S.H., F. Frigerio, M. Watanabe, F. Picard, M. Joaquin, M. Sticker, S. Fumagalli, P.R. Allegrini, S.C. Kozma, J. Auwerx, and G. Thomas. 2004. Absence of S6K1 protects against age- and diet-induced obesity while enhancing insulin sensitivity. *Nature.* 431:200–205. http://dx.doi.org/10.1038/nature02866

Um, S.H., M. Sticker-Jantscheff, G.C. Chau, K. Vintersten, M. Mueller, Y.G. Gangloff, R.H. Adams, J.F. Spetz, L. Elghazi, P.T. Pfluger, et al. 2015. S6K1 controls pancreatic β cell size independently of intrauterine growth restriction. *J. Clin. Invest.* 125:2736–2747. http://dx.doi.org/10.1172/JCI77030

Vergès, B., and B. Cariou. 2015. mTOR inhibitors and diabetes. *Diabetes Res. Clin. Pract.* 110:101–108. http://dx.doi.org/10.1016/j.diabres.2015.09.014

Wolfson, R.L., L. Chantranupong, R.A. Saxton, K. Shen, S.M. Scaria, J.R. Cantor, and D.M. Sabatini. 2016. Sestrin2 is a leucine sensor for the mTORC1 pathway. *Science.* 351:43–48. http://dx.doi.org/10.1126/science.aab2674

Xu, G., G. Kwon, W.S. Cruz, C.A. Marshall, and M.L. McDaniel. 2001. Metabolic regulation by leucine of translation initiation through the mTOR-signaling pathway by pancreatic β-cells. *Diabetes.* 50:353–360. http://dx.doi.org/10.2337/diabetes.50.2.353

Yano, M., K. Watanabe, T. Yamamoto, K. Ikeda, T. Senokuchi, M. Lu, T. Kadomatsu, H. Tsukano, M. Ikawa, M. Okabe, et al. 2011. Mitochondrial dysfunction and increased reactive oxygen species impair insulin secretion in sphingomyelin synthase 1-null mice. *J. Biol. Chem.* 286:3992–4002. http://dx.doi.org/10.1074/jbc.M110.179176

Zoncu, R., A. Efeyan, and D.M. Sabatini. 2011. mTOR: From growth signal integration to cancer, diabetes and ageing. *Nat. Rev. Mol. Cell Biol.* 12:21–35. http://dx.doi.org/10.1038/nrm3025